

MOLECULAR MECHANISMS OF ZEBRAFISH MOTONEURON DEVELOPMENT

by

LAURA ANN HALE

A DISSERTATION

Presented to the Department of Biology
and the Graduate School of the University of Oregon
in partial fulfillment of the requirements
for the degree of
Doctor of Philosophy

December 2009

University of Oregon Graduate School

Confirmation of Approval and Acceptance of Dissertation prepared by:

Laura Hale

Title:

"Molecular Mechanisms of Zebrafish Motoneuron Development"

This dissertation has been accepted and approved in partial fulfillment of the requirements for the Doctor of Philosophy degree in the Department of Biology by:

Monte Westerfield, Chairperson, Biology
Judith Eisen, Advisor, Biology
Victoria Herman, Member, Biology
John Postlethwait, Member, Biology
Clifford Kentros, Outside Member, Psychology

and Richard Linton, Vice President for Research and Graduate Studies/Dean of the Graduate School for the University of Oregon.

December 12, 2009

Original approval signatures are on file with the Graduate School and the University of Oregon Libraries.

© 2009 Laura Ann Hale

An Abstract of the Dissertation of

Laura Ann Hale for the degree of Doctor of Philosophy
in the Department of Biology to be taken December 2009

Title: MOLECULAR MECHANISMS OF ZEBRAFISH MOTONEURON
DEVELOPMENT

Approved: _____
Dr. Judith Eisen

This dissertation describes research to identify genes involved in specification, patterning and development of zebrafish primary motoneurons. We first examined the spatiotemporal expression patterns of retinoic acid and retinoid X receptor mRNAs to determine whether particular ones might be involved in motoneuron specification or patterning. Retinoic acid and retinoid X receptor mRNAs are expressed at the right time to pattern motoneurons, but the expression patterns did not suggest roles for particular receptors. In contrast, netrin mRNAs are expressed in specific motoneuron intermediate targets and knockdown experiments revealed an important role in development of VaP motoneurons. Two identified motoneurons, CaP and VaP, initially form an equivalence pair. CaPs extend long axons that innervate ventral muscle. VaPs extend short axons that stop at muscle fibers called muscle pioneers; VaPs later typically die. Previous work showed that during extension, CaP axons pause at several intermediate targets, including muscle pioneers, and that both CaP and muscle pioneers are required for VaP formation. We found that mRNAs for different Netrins are expressed in intermediate targets before CaP axon

contact: *netrin 1a* in muscle pioneers, *netrin 1b* in hypochord, and *netrin 2* in ventral somite. We show that Netrins are unnecessary to guide CaP axons but are necessary to prevent VaP axons from extending into ventral muscle. Netrin 1a is necessary to stop VaP axons at muscle pioneers, Netrin 1a and Netrin 2 together are necessary to stop VaP axons near the hypochord, and Netrin 1b appears dispensable for CaP and VaP development. We also identify Deleted in colorectal carcinoma as a Netrin receptor that mediates the ability of Netrin 1a to cause VaP axons to stop at muscle pioneers. Our results suggest Netrins refine axon morphology to ensure final cell-appropriate axon arborization. To learn whether Netrin proteins diffuse away from their sources of synthesis to function at a distance, we are developing Netrin antibodies. If successful, the antibodies will provide the research community at large with a new tool for understanding in vivo Netrin function.

This dissertation includes both my previously published and unpublished coauthored material.

CURRICULUM VITAE

NAME OF AUTHOR: Laura Ann Hale

PLACE OF BIRTH: Misawa Air Force Base, JAPAN

DATE OF BIRTH: June 16, 1978

GRADUATE AND UNDERGRADUATE SCHOOLS ATTENDED:

University of Oregon, Eugene

University of California, Berkeley

DEGREES AWARDED:

Doctor of Philosophy, Biology, 2009, University of Oregon, Eugene

Bachelor of Arts, Molecular and Cell Biology and Psychology, 2001, University of California, Berkeley

AREAS OF SPECIAL INTEREST:

Neuroscience

Developmental Biology

PROFESSIONAL EXPERIENCE:

Graduate Teaching Fellow, UO Biology Dept., 2004

Research Assistant, UCB Psychology Dept., Dr. R.T. Knight, 2001-03

Research Assistant, UCB Mol. & Cell Biology Dept., Dr. F.H. Wilt, 2000-01

Undergraduate Student Instructor, UCB Integrative Biology Dept., 1998

Tutor, UCB College Writing Dept., 1997

GRANTS, AWARDS AND HONORS:

Northwest Regional Developmental Biology Conference, 2nd place, Student Oral Presentation, 2009

UO Clarence and Lucille Dunbar Scholarship Recipient, 2007-08

Caswell Grave Scholarship, Embryology, Marine Biological Laboratory, Wood Hole, MA, 2007

John & Madeleine Trinkaus Endowed Scholarship, Embryology, Marine Biological Laboratory, Wood Hole, MA, 2007

American Heart Association Predoctoral Fellow, 2006-08

NIH Genetics Training Grant Appointee, 2004-05, 08-09

UCB Biology Fellows Program Research Grant Recipient, 2001

PUBLICATIONS:

- Solbakk, A.K., Alpert, G.F., Furst, A.J., Hale, L.A., Oga, T., Chetty, S., Pickard, N., Knight R.T. (2008) Altered prefrontal function with aging: insights into age-associated performance decline. *Brain Res.* 1232:30-47.
- Hutchinson, S.A., Cheesman, S.E., Hale, L.A., Boone, J.Q., Eisen, J.S. (2007) Nkx6 proteins specify one zebrafish primary motoneuron subtype by regulating late *islet1* expression. *Development* 134(9):1671-7.
- Padilla, M.L., Wood, R.A., Hale, L.A., Knight, R.T. (2006) Lapses in a prefrontal-extrastriate preparatory attention network predict mistakes. *J. Cogn. Neurosci.* 18(9):1477-87.
- Hale, L.A.* , Tallafuss, A.* , Yan, Y.L., Dudley, L., Eisen, J.S., Postlethwait, J.H. (2006) Characterization of the retinoic acid receptor genes *raraa*, *rarab* and *rarg* during zebrafish development. *Gene Expr. Patterns* 6(5):546-55.
- Tallafuss, A.* , Hale, L.A.* , Yan, Y.L., Dudley, L., Eisen, J.S., Postlethwait, J.H. (2006) Characterization of retinoid-X receptor genes, *rxra*, *rxrba*, *rxrbb* and *rxrg*, during zebrafish development *Gene Expr. Patterns* 6(5):556-6).
- Tanaka, M., Hale, L.A., Amores, A., Yan, Y.L., Cresko, W.A., Suzuki, T., Postlethwait, J.H. (2005) Developmental genetic basis for the evolution of pelvic fin loss in the pufferfish *Takifugu rubripes*. *Dev Biol.* 281(2):227-39.
- Yamaguchi, S., Hale, L.A., D'Esposito, M., Knight, R.T. (2004) Rapid prefrontal-hippocampal habituation to novel events. *J. Neurosci.* 24: 5356-5363.

* Authors contributed equally to this work

ACKNOWLEDGEMENTS

The collaborative and nurturing environment of the University of Oregon's Institute of Neuroscience enabled me to successfully complete my dissertation research. I am fortunate to be able to consider my colleagues friends. I thank Dr. Judith Eisen for sharing her gift for story-telling; I hope to convey the complexities of developmental neurobiology as compellingly and simply. I am also grateful for her generous open office door policy. Dr. John Postlethwait patiently supported and guided me while I chose a dissertation lab and throughout my graduate career. I appreciate Dr. Monte Westerfield's insightful questions that helped me to delve deeper into my research. Similarly, Dr. Tory Herman's questions provided a more critical perspective of my work. I thank Dr. Cliff Kentros for providing an alternate viewpoint of my work. I also wish to thank Dr. Yasuko Honjo for her patient training and prodding me to think more critically. I am grateful to the Institute of Neuroscience staff, especially Ellen McCumsey, Peg Morrow, Mike McHorse, Don Pate and Mikel Rhodes, and the biology staff, especially Donna Overall, for their excellent administrative and technical support. I thank the University of Oregon Zebrafish Facility for fish husbandry.

Dr. Chi-Bin Chien and his lab at the University of Utah generously provided reagents and advice for the Netrin project. This work was supported by AHA 0610097Z, NIH GM07413 and NIH NS23915.

Finally, I am deeply indebted to Bill Gillis for his unwavering support.

For Chen Hale and Johnathan Hale

TABLE OF CONTENTS

Chapter	Page
I. INTRODUCTION	1
II. CHARACTERIZATION OF THE RETINOIC ACID RECEPTOR GENES <i>RARAA</i> , <i>RARAB</i> AND <i>RARG</i> DURING ZEBRAFISH DEVELOPMENT	4
1. Results and Discussion	4
1.1. Orthologies of Zebrafish <i>rar</i> Genes	5
1.2. Expression of <i>rar</i> Genes During Zebrafish Embryonic Development	9
1.2.1. Maternal Expression of <i>rar</i> Genes	9
1.2.2. <i>raraa</i> Expression	12
1.2.3. <i>rarab</i> Expression	16
1.2.4. <i>rarg</i> Expression	18
1.3. Conclusions	20
2. Experimental Procedures	20
2.1. Cloning of <i>rar</i> Genes	20
2.2. Whole Mount In Situ Hybridization	21
2.3. Sources of Additional Gene Expression Data	21
III. CHARACTERIZATION OF RETINOID-X RECEPTOR GENES <i>RXRA</i> , <i>RXRBA</i> , <i>RXRBB</i> AND <i>RXRG</i> DURING ZEBRAFISH DEVELOPMENT	23
1. Results and Discussion	23
1.1. Orthologies of Zebrafish <i>rxr</i> Genes	24

Chapter	Page
1.2. Expression of <i>rxr</i> Genes During Zebrafish Embryonic Development	28
1.2.1. Maternal Expression of <i>rxr</i> Genes	31
1.2.2. <i>rxra</i> Expression	32
1.2.3. <i>rxrba</i> and <i>rxrbb</i> Expression	32
1.2.4. <i>rxrg</i> Expression	36
1.2.5. Comparison of Zebrafish <i>rxr</i> Genes	37
1.2.6. Comparison to <i>Rxr</i> Gene Expression in Mouse and Chick	39
1.3. Conclusions	40
2. Experimental Procedures	41
2.1. Cloning of <i>rxr</i> Genes	41
2.2. Whole Mount RNA In Situ Hybridization	41
2.3. Sources of Additional Gene Expression Data	42
IV. NETRIN SIGNALING IS REQUIRED FOR DEVELOPMENT OF AN IDENTIFIED ZEBRAFISH MOTONEURON	44
Summary	44
Introduction	44
Materials and Methods	47
Results	51
Discussion	62
Conclusion	67

Chapter	Page
V. CONCLUSION.....	69
REFERENCES.....	71

LIST OF FIGURES

Figure	Page
Chapter II	
1. Phylogeny of Retinoic Acid Receptor Proteins	7
2. Conserved Syntenies for <i>Rar</i> Genes.....	10
3. <i>raraa</i> , <i>rarab</i> and <i>rarg</i> Expression Visualized at 1.5-2, 4.7, 9 and 10.5-11 hpf	12
4. <i>raraa</i> , <i>rarab</i> and <i>rarg</i> Transcript Expression Visualized at 12, 24 and 48 hpf	14
5. Distinctive Expression of <i>raraa</i> , <i>rarab</i> and <i>rarg</i>	15
Chapter III	
1. Phylogenetic Analysis of Retinoid-X Receptor Proteins	27
2. Genomic Analysis of Conserved Syntenies for Zebrafish <i>rxra</i> and <i>rxrg</i> Genes.....	29
3. Genomic Analysis of Conserved Syntenies for Zebrafish <i>RXRB</i> Co-Orthologs	31
4. Expression of <i>rxra</i> , <i>rxrba</i> , <i>rxrbb</i> and <i>rxrg</i> Visualized at 1.5-2, 4.7, 8-9 and 10.5-11 hpf	33
5. Expression of <i>rxra</i> , <i>rxrbb</i> and <i>rxrg</i> at 12, 24 and 48 hpf.....	34
6. Distinctive Expression of <i>rxra</i> , <i>rxrbb</i> and <i>rxrg</i>	35
Chapter IV	
1. Netrin mRNAs Are Expressed at Intermediate Targets for the CaP Axon.....	52
2. Netrins Are Unnecessary for CaP Axons to Extend into Ventral Muscle	54
3. Ntn1a Is Necessary for VaP Axons to Stop at the Horizontal Myoseptum	57

Figure	Page
4. Netrins Act Together to Restrict Extension of a Second CaP Axon into Ventral Muscle.....	60
5. Dcc Is Necessary for VaP Axons to Stop at Muscle Pioneers.....	61

LIST OF TABLES

Table	Page
Chapter II	
1. Survey of Recent and Previous <i>Rar</i> Gene Names.....	6
Chapter III	
1. Survey of Recent and Previous <i>Rxr</i> Gene Names.....	26
2. Primer Sequences Used to Obtain <i>rxr</i> Clones.....	42
Chapter IV	
1. MO Sequences Used to Knock Down Netrins and Dcc and RT Primer Sequences Used to Confirm MO Efficacy	49
2. Netrin Signaling Is Necessary to Prevent a Second CaP Axon from Extending into Ventral Muscle.	64

CHAPTER I

INTRODUCTION

Analyzing neurodevelopment to understand the origins of behavior

What are the origins of behavior? Approaches for answering that question range from analyzing macroscopic observations of people behaving under various conditions to analyzing microscopic observations of individual neurons believed to contribute to the neural circuitry of readily identifiable behaviors. Collectively, each approach informs the other. For example, studying people as they behave while monitoring their brain activity with various neuroimaging techniques enables researchers to identify brain regions involved in generating behaviors. Researchers interested in determining neural circuitry underlying behavior can then study neurons in brain regions identified by macroscopic approaches to confirm whether they contribute to behavior. Molecular approaches to understanding behavior also inform macroscopic approaches to behavior. Knockdown analysis of genes that lead to behavioral deficits can help identify specific neurons and brain regions that generate behavior. In this dissertation, I describe work that contributes to determining genes involved in the development of a neural circuit responsible for motility.

Patterning the vertebrate nervous system

I studied genes involved in patterning zebrafish spinal cord during development as a model for understanding how neuronal identity might be conferred in vertebrates with larger central nervous systems; the relatively small size of the zebrafish nervous system provides an excellent system for understanding neurodevelopment at the level of individual neurons. If

neuronal subpopulations are not correctly specified then these components of a neural circuit will likely not function correctly to generate behavior.

Patterning of the nervous system begins along the rostrocaudal axis and then extends along the dorsoventral axis. Within the developing vertebrate spinal cord, Sonic hedgehog protein released from the notochord serves as a ventralizing signal, diffusing from its source to create a gradient of expression. Cells exposed to different concentrations of Sonic hedgehog adopt different neuronal fates. For example, cells adjacent to the notochord adopt floorplate identity and later, more distant cells adopt motoneuron fates [reviewed by (Concordet and Ingham, 1995)]. Retinoic acid signaling also acts to pattern the nervous system along the rostrocaudal and dorsoventral axes (Maden, 2002). Retinoic acid signaling is also implicated in specification and differentiation of motoneurons (Maden, 2002; Appel and Eisen, 2003; Sockanathan et al., 2003; Begemann et al., 2004; Linville, 2004; Goncalves et al., 2005).

Two distinct populations of motoneurons, primary motoneurons and secondary motoneurons, arise from the motoneuron progenitor domain in zebrafish. Primary motoneurons are born earlier and are less numerous than secondary motoneurons. I studied the role of retinoic acid signaling in patterning motoneurons by analyzing expression of retinoic acid receptor and their potential binding partners, retinoid X receptors. I describe this work in Chapters II and III; both chapters include material coauthored with A. Tallafuss, Y.L. Yan, L. Dudley, J.H. Postlethwait, and J.S. Eisen.

Connecting neurons to their targets

I also studied how individual motoneurons connect to their muscle targets. Studying which genes are required for appropriate motoneuron and muscle connectivity in the

peripheral nervous systems provides insight into how neurons within the central nervous system may be wired together during development. Building connections between neurons and an inappropriate target would likely generate an improperly wired circuit incapable of producing behavior. Attempts to answer how connections between neurons and their often distant targets are established during development have led to the now familiar axon guidance molecule, Netrin-1. The axonal pathway development of commissural neurons, an interneuron subpopulation whose cell bodies lie within the dorsal spinal cord and whose axons extend across the ventral midline, has been used as a model for studying axon guidance. In zebrafish, Netrins may function to guide a class of ventrally projecting motoneurons to their muscle targets. I discuss the results of this work in Chapter IV.

Finally, I conclude in Chapter V with a brief discussion about the implications of my dissertation research.

CHAPTER II
CHARACTERIZATION OF THE RETINOIC ACID RECEPTOR GENES
***RARAA*, *RARAB* AND *RARG* DURING ZEBRAFISH DEVELOPMENT**

The work described in this chapter was previously published in “Gene Expression Patterns,” Vol. 6. I share first authorship with A. Tallafuss. We were responsible for the majority of data collection, data analysis and writing. Y.L. Yan and L. Dudley cloned *rarg*. J.H. Postlethwait completed the syntenic analysis and contributed to writing. J.S. Eisen also contributed to writing.

1. Results and discussion

Retinoic acid receptors (Rars) and retinoid-X receptors (Rxrs) form retinoic acid (RA) activated heterodimers that bind retinoic acid response elements (RAREs) and modulate transcription of target genes [reviewed by (Bastien and Rochette-Egly, 2004)]. In zebrafish as well as in tetrapod vertebrates, RA controls patterning of the central nervous system (CNS), paired appendages, and other organs (Gavalas and Krumlauf, 2000; Grandel et al., 2002; Jiang et al., 2002), as demonstrated by the characterization of embryos homozygous for mutations altering *Raldh2*, the enzyme required for RA synthesis (Begemann et al., 2001; Niederreither et al., 1999). Furthermore, mutations in RARs can lead to cancers such as acute promyelocytic leukemia or to heart malformations, and aberrant RA signaling may contribute to Parkinson’s disease and schizophrenia (Krezel et al., 1998; Soprano and Soprano, 2002; Lane and Bailey, 2005; Goodman, 2005; Rioux and Arnold, 2005). RA is important for somite formation (Appel and Eisen, 2003) and also plays

a role in patterning both the anterioposterior and dorsoventral axes of the CNS (Maden, 2002) with primary sites of action in the hindbrain and anterior spinal cord (Maden, 2002). RA is also implicated in specification and differentiation of motoneurons (Maden, 2002; Appel and Eisen, 2003; Sockanathan et al., 2003; Begemann et al., 2004; Linville, 2004; Goncalves et al., 2005) and interneurons (Maden, 2002). Three *Rar* genes (*Rara*, *Rarb*, and *Rarg*) have been isolated from tetrapods (<http://www.ncbi.nlm.nih.gov/entrez/query.fcgi?db=gene>). In cultured neural progenitor cells, the order and combination of Rar activation determines the type of neural cells that are generated (Goncalves et al., 2005), suggesting that different Rars may play distinct roles during development. Although three *rar* genes have been isolated in zebrafish (White et al., 1994; Joore et al., 1994), there has yet to be a thorough study of their orthologies, genomic arrangements, and embryonic expression patterns. As a necessary precursor to understanding the roles of Rars in cell specification during zebrafish development, we have investigated the orthologous relationships and expression patterns of three zebrafish *rar* genes.

1.1. Orthologies of zebrafish *rar* genes

To make meaningful comparisons of zebrafish gene expression patterns to those of mouse and other tetrapods, it is essential to evaluate orthologous genes. Phylogenetic analysis of zebrafish Rars (Fig. 1) showed that sequences L03398 and L03399 (formerly called *rara2a* and *rara2b* (Mangelsdorf et al., 1995) grouped as co-orthologs of tetrapod *Rara* proteins with high bootstrap support. Thus, these genes should be renamed *raraa* and *rarab* according to zebrafish nomenclature rules (http://zfin.org/zf_info/nomen.html); refer also to Table 1. We found an ortholog of *raraa* in the pufferfish genome, but not an ortholog of

rarb (Fig. 1). Although no *rarb*-like sequence has been described in zebrafish, or located in the Zv4 or Zv5 assembly of the zebrafish genome

(http://www.ensembl.org/Danio_rerio/index.html), we identified a sequence in the pufferfish genome that fell in the tree as expected for an ortholog of mammalian *Rarb* (Fig. 1). We do not know whether the zebrafish genome lacks a *rarb* gene or if we were unable to identify it. Mice lacking *Rarb* function grow slowly, but are otherwise apparently normal (Ghyselinck et al, 1997).

The tree further showed that zebrafish and pufferfish both have an ortholog of human *RARG* (Fig. 1). Phylogenetic analysis indicated that *RAR* genes are more closely related to *thyroid hormone receptor* genes (*THR*s), which are their near neighbors on human chromosomes, than to the genes encoding the *RXR*s with which they functionally interact.

Table 1. Survey of recent and previous *Rar* gene names.

Zebrafish Gene	Accession number	Previous Zebrafish Gene	Human Ortholog	Mouse ortholog
<i>raraa</i> *	<u>L03398</u>	<i>zRARα¹; rara2α²</i>	<i>RARA</i> ⁴	<i>Rara</i> ⁵
<i>rarab</i> *	<u>L03399</u>	<i>rarab</i> ² ; <i>rara2b</i> ³		
none identified*		none identified	<i>RARB</i> ⁴	<i>Rarab</i> ⁵
<i>rarg</i> *	<u>S74156</u>	<i>zRARγ¹; rarg</i> ^{2,3}	<i>RAR</i> ⁴	<i>Rarg</i> ⁵

*this paper

¹Joore et al., 1994

²Strausberg et al., 2002

³ZFIN (2003; <http://zfin.org/cgi-bin/webdriver?MIval=aa-pubview2.apg&OID=ZDB-PUB-030508-1>)

⁴HUGO (2005; <http://www.gene.ucl.ac.uk/nomenclature/index.html>)

⁵MGI (2005; <http://www.informatics.jax.org/>)

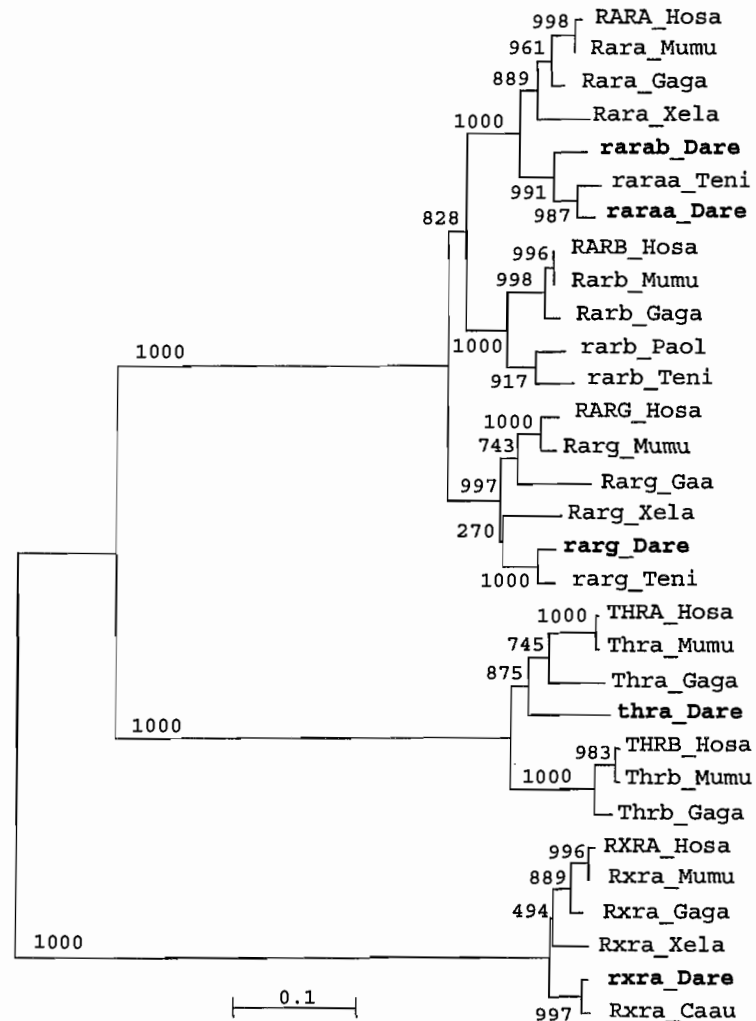


Fig. 1. Phylogeny of retinoic acid receptor proteins. Amino acid sequences were aligned by Clustal-X, sequences were trimmed to include unambiguously aligned regions, and phylogenetic analysis was by the neighbor-joining method (Saitou, 1987). Numbers are bootstraps values out of 1000 runs. Alignments are available on request. Species abbreviations: Hosa, *Homo sapiens* (human); Mumu, *Mus musculus* (mouse); Gaga, *Gallus gallus* (chicken); Xela, *Xenopus laevis* (frog); Dara, *Danio rerio* (zebrafish); Paol, *Paralichthys olivaceus* (flounder); Teni, *Tetraodon nigroviridis* (pufferfish); Caau, *Carassius auratus* (goldfish). Sequence accession numbers: RARA Hosa AAB19602; Rara Mumu AAH10216; Rara Gaga CAA55134; Rara Xela A56558; rarab Dare AAH49301; raraa Teni GSTENT00024106001; raraa Dare NP 571481; RARB Hosa AAH60794; Rarb Mumu NP 035373; Rarb Gaga CAA39997; rarb Paol BAB71757; rarb Teni CAG11671; RARG Hosa CAB60726; Rarg Mumu P20787; Rarg Gaga CAA52153; Rarg Xela P28699; rarg Dare Q91392; rar Teni GSTENT00021064001; THRA Hosa 135702; Thra Mumu 586089; Thra Gaga NP_990644; thra Dare 1314773; THRB Hosa P37243; Thrb Mumu NP_033406; Thrb Gaga CAA90566; RXRA Hosa NP_002948; Rxra Mumu AAB36778; Rxra Gaga XP_415426; Rxra Xela P51128; rxraa Dare ENSDARP00000003080; Rxra Caau AAO22211.

Analysis of conserved synteny can provide evidence of orthologies independent of recent phylogenies and is necessary to determine whether the duplicated genes *raraa* and *rarab* are tandem duplicates or if they arose in the ancient teleost genome duplication (Amores et al, 1998; Postlethwait et al., 1998; Woods et al., 2000; Taylor et al., 2003). Zebrafish co-orthologs of *RARA* reside in conserved chromosome segments on the duplicated linkage groups LG3 and LG12 (Fig. 2A1, 2A6), with *raraa/RARA* and *top2a/TOP2A* near neighbors in zebrafish and human genomes (Fig. 2A2-4), and *rarab* just three genes from an ortholog of *NBR1* which resides about 2Mb from *RARA* (Fig. 2A3, 2A5). (Note that *Zv4* has *raraa* incorrectly positioned on Chromosome 18). The analysis of orthologous relationships confirms the decision to rename the zebrafish sequences *raraa* and *rarab* based on phylogenetic analyses and shows that *raraa* and *rarab* arose in the teleost genome duplication event. Although we found in *Zv4* the zebrafish orthologs of *TOP2B* and *THRB*, which flank *RARB* in human, these genes were dispersed in the zebrafish genome and are not located near any *RAR*-like sequence. In contrast, we found the ortholog of *RARB* (GSTENT00033708001) in the genome of the pufferfish *Tetraodon nigroviridis* next to the pufferfish ortholog of *TOP2B* (Fig. 2B), confirming orthologies shown in the tree (Fig. 1). We suggest that chromosome rearrangements that dispersed the neighbors of *rarb* may have led to its loss from the zebrafish genome. The zebrafish sequence Q91392 mapped to LG23 (Fig. 2C1) and it resides in the genome near several other loci whose human orthologs are near *RARG* on human (*Homo sapiens*, Hosa) chromosome Hosa12q13 (Fig. 2C3, 2C4). These comparative synteny data provide strong evidence that *rarg* is the ortholog of tetrapod *RARG*. The close linkage of paralogs of *RAR*, *THR*, *TOP2*, and *HOX* genes in the human genome is consistent with the origin of the three human *RAR* genes by chromosome (or

genome) duplication at the base of vertebrate evolution, and the origin of *rara* paralogs in zebrafish by an additional genome duplication event in ray fin fish evolution.

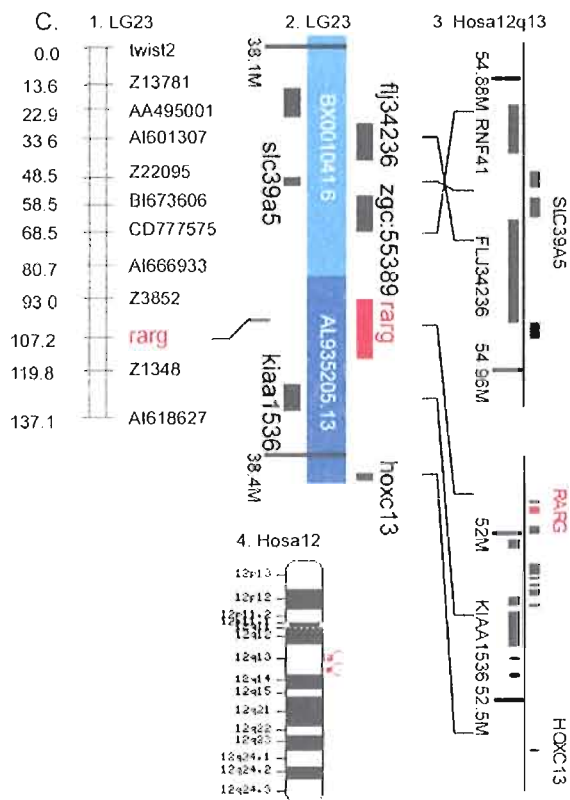
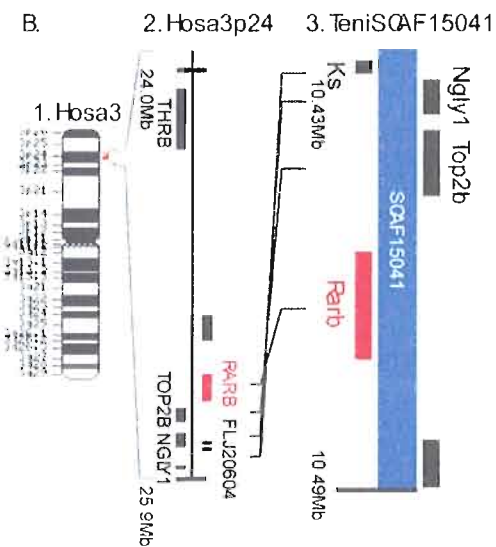
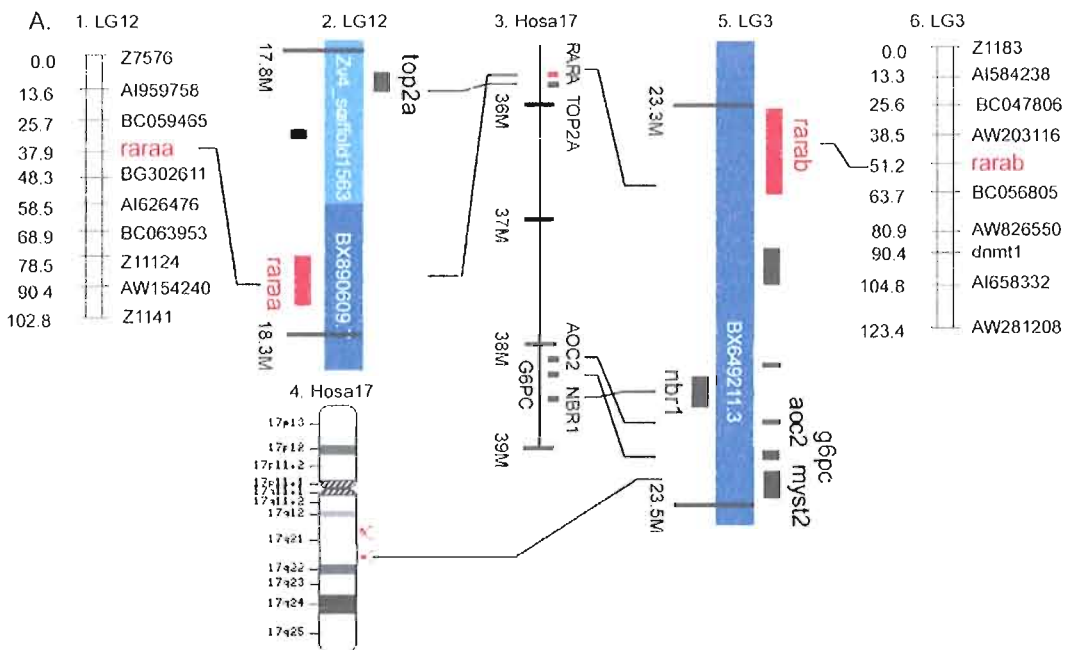
1.2. Expression of *rar* genes during zebrafish embryonic development

We assayed the temporal and spatial distribution of *raraa*, *rarab* and *rarg* by whole mount RNA in situ hybridization beginning in the cleavage period (0.75-2 hours post fertilization, hpf), extending through the blastula (2.25-4.66 hpf), gastrula (5.25-10 hpf), segmentation (10.33 -22 hpf), and pharyngula (24-42 hpf) stages and concluding in the hatching period (48-72 hpf). For the purpose of comparison, Fig. 3 and 4 contain overviews of *rar* expression and Fig. 5 details unique *rar* expression patterns in the head and tail.

1.2.1. Maternal expression of *rar* genes

In situ hybridization experiments revealed *rarab* and *rarg* transcripts during cleavage (1.5 hpf; Fig. 3B) and blastula stages (4.7 hpf; 3C). Because early *rarab* expression was similar to *rarg* expression, we show only one example of expression for each gene at early developmental stages (Fig. 3B, 3C). Consistent with previous results (Joore et al., 1994) and in comparison to embryos treated with a *raraa* sense probe, we did not observe *raraa* expression at 1.5 hpf (Fig. 3A) and 4.7 hpf (data not shown); expression of *raraa* was not observed until 8 hpf. In addition, we did not observe localized *rar* expression patterns (described below) until later gastrula stages.

Fig. 2. Conserved synteny for *Rar* genes. A. Mapping and local conserved synteny for zebrafish *raraa* and *rarab* show that these genes reside in duplicated chromosome segments. B. A *Rarb*-like sequence in the genome of the pufferfish *Tetraodon nigroviridis* resides immediately adjacent to orthologs of genes that are adjacent to *RARB* in human, but orthologous sequences were not found in the zebrafish genome. C. Mapping and local conserved synteny for zebrafish *rarg* shows that it resides near genes that are near *ARG* in human. In A2, *raraa* is ENSDART00000026235 and *top2a* is ENSDART00000050143. In A5, *rarab* is ENSDART00000044677; *gopc* is ENSDART00000014812; *myst2* is ENSDART00000049095; *nbr1* is ENSDART00000018647; and *aoc2* is ENSDART00000027258. In B3, *Rarb* is GSTENT00033708001; *Top2b* is GSTENT00033707001; *Ngly1* is GSTENT00033706001; and *Ks* is GSTENT00033705001. In C2, *rarg* is ENSDARESTT00000015370; *kiaa1536* is ENSDART00000040596; *slc39a5* is ENSDART00000029724; *flj34236* is ENSDART00000042557; *zgc:55389* is ENSDART00000016912; and *hoxc13* is ENSDART00000017685.



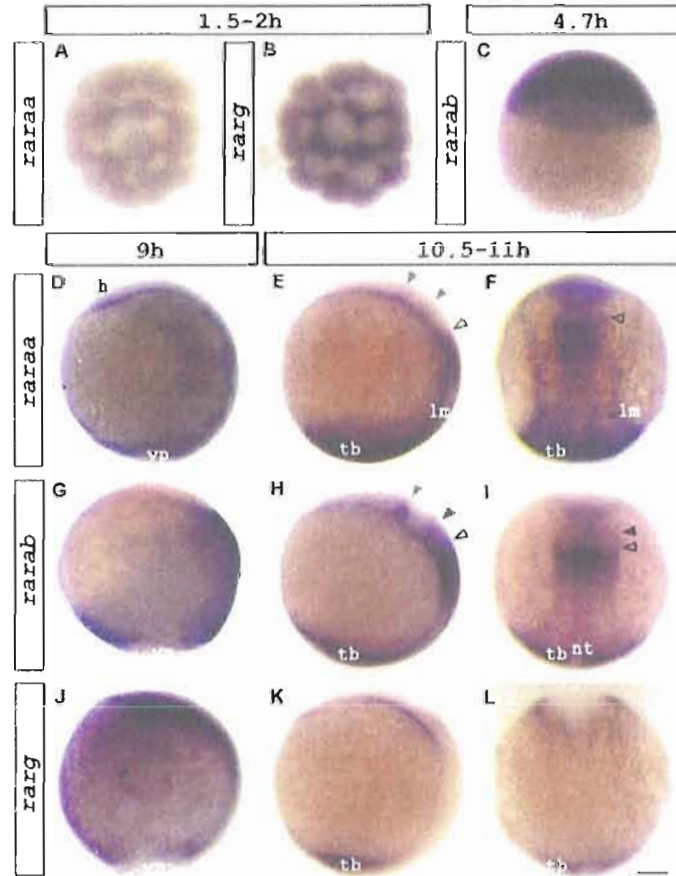


Fig. 3. *raaa* (A, D-F), *rarab*, (C, G-I), and *rarg* (B, J-L) expression visualized at 1.5-2 hpf (A,B), 4.7 hpf (C), 9 hpf (D,G,J) and 10.5-11 hpf (E,F,H,I,K,L). Dorsal view (A,B,F,I,L). Lateral view; anterior up and dorsal to the left (D,E,G,H,J,K). (E) Grey arrowheads mark narrow anterior bands. Open black arrowhead marks posterior broad band. (H) Grey arrowhead marks single anterior band. Black arrowhead marks faint broad band. Open black arrowhead marks prominent broad band. Abbreviations: h, presumptive head; lm, lateral mesoderm; nt, notochord; tb, tailbud; v, vegetal pole; yp, yolk plug. Scale bar represents 118 μ m in 2A, 2B, 135 μ m in 2C, and 121 μ m in 2D-L.

1.2.2. *raaa* expression

At 9 hpf, *raaa* transcripts were expressed throughout the dorsal epiblast (Fig. 3D), except in the dorsal midline (data not shown), and were expressed ventrally, in prospective head and tail regions (Fig. 3D). Expression of *raaa* was further restricted during the segmentation period.

At the beginning of segmentation (10-11 hpf), *raraa* was expressed in the presumptive hindbrain, posterior neural plate and tail region (Fig. 3E). Expression of *raraa* within the neural plate extended in a gradient along the anterioposterior axis (Fig. 3F); the strongest expression occurred anteriorly in the hindbrain and posteriorly in the tailbud. In the hindbrain (Fig. 3F), *raraa* was expressed in three stripes perpendicular to the anterioposterior axis: two faint, narrow, anterior bands (grey arrowheads in Fig. 3E) and a strong, broad, posterior band that faded posteriorly (open arrowhead in Fig. 3E). Intense *raraa* staining also appeared in the tail bud and in lateral mesoderm (Fig. 3E, 3F). RNA in situ hybridization experiments with *egr2b* (*krox20*), a gene expressed in hindbrain rhombomeres 3 and 5, revealed that the two narrow bands of *raraa* expression (grey arrowheads in Fig. 3E) were anterior to rhombomere 3 (data not shown), whereas the anterior border of the single broad band (open arrowhead in Fig. 3E) lay within rhombomere(s) 6 and/or 7 (Fig. 5A, 5B).

At 12 hpf, expression of *raraa* in the head and tail remained similar to that observed in earlier segmentation stages (Fig. 4A). Expression lateral to the presumptive spinal cord present earlier had disappeared by 11 hpf. We observed additional *raraa* expression in the eyes and in tissue adjacent to the two faint narrow stripes described above (Fig. 4A, see also Joore et al., 1994). The distribution of *Rara* transcripts during neural tube formation in mouse embryos (Ruberte et al., 1993) is similar to the expression of *raraa* in zebrafish embryos. Both mouse *Rara* (Ruberte et al., 1993) and zebrafish *raraa* are expressed strongly anteriorly.

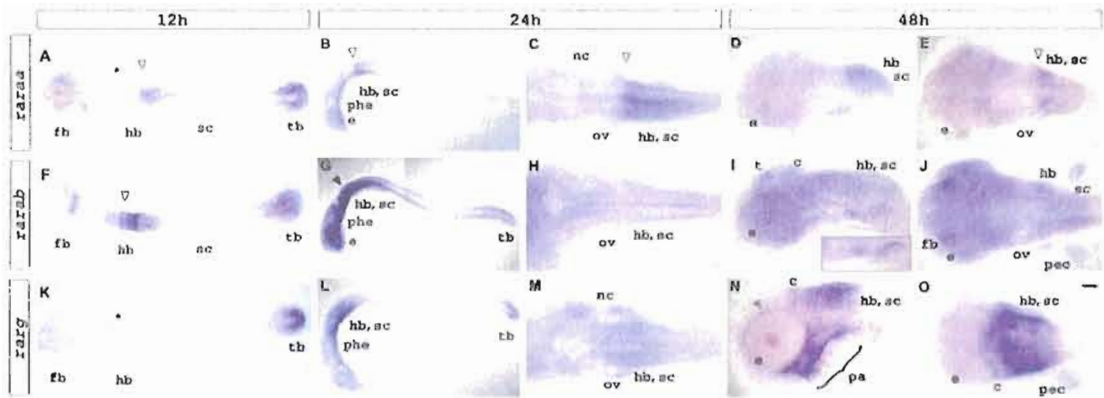


Fig. 4. *raraan* (A-E), *rarab* (F-J) and *rarg* (K-O) transcript expression visualized at 12 hpf (A,F,K), 24 hpf (B,C,G,H,L,M) and 48 hpf (D,E,I,J,N,O). Refer to text for detailed descriptions. Flat-mount embryos seen from a dorsal view (A,C,E,F,H,J,K,M,O) or a lateral view (B,D,G,I,L,N). Anterior is to the left. (A) Asterisk marks expression in two stripes lateral to the neural tube. (A-C) Open black arrowhead marks broad stripe of *raraan* hindbrain expression. (F,G) Open black arrowhead marks broad stripe of *rarab* hindbrain expression. (I) Inset shows a magnified view of *rarab* expression in the pharyngeal region. (K) Asterisk marks anterior lateral mesenchyme. (N) Grey arrowhead marks staining around eye. Abbreviations: c, cerebellum; e, eye; fb, forebrain; hb, hindbrain; nc, neural crest; ov, otic vesicle; pec, pectoral fin bud; pa, pharyngeal arches; phe, pharyngeal endoderm; sc, spinal cord; t, tectum; tb, tailbud. Scale bar represents 115 μ m in 4A,F,K; 100 μ m in 4B,G; 90 μ m in 4L; 42 μ m in 4C,H; 35 μ m in 4D,E,I,J,N,O; 33 μ m in 4M.

During the segmentation period, *raraan* was expressed in both neural and underlying non-neural tissue (Fig. 4A-C), but was lost in the tailbud by 24 hpf (Fig. 4B). At 24 hpf, *raraan* expression was mostly restricted to the hindbrain and anterior spinal cord (Fig. 4B, 4C). Neural expression of *raraan* was localized in the hindbrain using mRNA expression of *egr2b* and the otic vesicle as positional markers. A faint band of *raraan* expression was located within rhombomere 3 and/or 4 (black arrowheads in Fig. 5C, 5D) and a sharp anterior border of *raraan* expression at the boundary of rhombomeres 6 and 7 (open black arrowheads in Fig. 5C, 5D). In the spinal cord, *raraan* expression at 24 hpf was graded along the anterioposterior and dorsoventral axes (Fig. 4B; see also Joore et al., 1994). In non-neural tissue, we found *raraan* expression in the pharyngeal endoderm and posterior neural crest population (Fig. 4B, 4C).

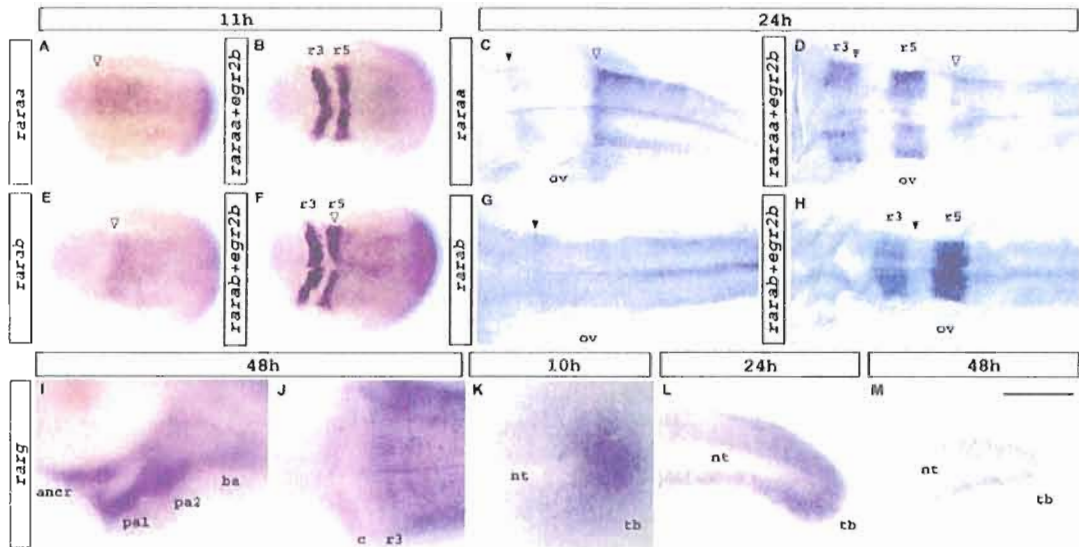


Fig. 5. Distinctive expression of *raraa* (A-D), *rarab* (E-H) and *rarg* (I-M). Refer to text for detailed descriptions. Anterior is to the left. Whole-mount embryos viewed dorsally (A,B,E,F). Flat-mount embryos seen from a dorsal view (C,D,G,H,J,K) or a lateral view (I,L,M). *raraa* expression and *egr2b* expression in the hindbrain at 11 hpf (A,B) and 24 hpf (C,D). Open black arrowhead marks anterior boundary of *raraa* expression in the posterior hindbrain (A,C,D). *rarab* and *egr2b* expression in the hindbrain at 11 hpf (E,F) and 24 hpf (G,H). Open black arrowhead marks anterior boundary *rarab* expression in the posterior hindbrain (E,F). Arrowhead marks the anterior boundary *rarab* expression in medial hindbrain (G,H). Magnified view of *rarg* expression in the neurocranium and arches (I) and hindbrain striping (J) at 48 hpf. *rarg* tail expression at 10 hpf (K), 24 hpf (L) and 48 hpf (M). Abbreviations: anc, anterior neurocranium; ba, branchial arches; c, cerebellum; nt, notochord; ov, otic vesicle; pa1, pharyngeal arch 1; pa2, pharyngeal arch 2; r3, rhombomere 3; r5, rhombomere 5; tb, tailbud. Scale bar represents 356 μm in 5A,B,E,F; 321 μm in 5C,D,G,H; 51 μm in 5I; 73 μm in 5J; 16 μm in 5K; 88 μm in 5L,M.

At 48 hpf, the posterior *raraa* hindbrain expression was the same as that observed at earlier stages (Fig. 4D, 4E; the anterior border of hindbrain expression was marked by an open black arrowhead). Expression in non-neural tissue was diffuse in the pharyngeal region. We detected restricted *raraa* expression in a lateral and ventral region posterior to the otic vesicle and anterior to the segmented mesoderm (Fig. 4D, 4E).

1.2.3. *rarab* expression

In late gastrula embryos (9 hpf), *rarab* expression was present in the dorsal epiblast and presumptive tail regions but expression was otherwise absent in the ventral epiblast (Fig. 3G). In contrast to *raraa* expression, which was broader and was excluded from only the ventral-most epiblast, *rarab* expression was limited to the dorsal region of the epiblast. By about 10 hpf, three distinct bands of *rarab* expression perpendicular to the anterioposterior axis appeared in the head: a narrow anterior band (grey arrowhead in Fig. 3H) and two broad posterior bands (black and open black arrowheads in Fig. 3H, 3I). The narrow anterior band (grey arrowhead in Fig. 3H) was located ventrally in the presumptive diencephalon. To determine the position of the *rarab* expression within the presumptive hindbrain, we performed one-color-double in situ hybridization experiments with *egr2b*. The boundary of the more anterior broad band (black arrowhead in Fig. 3H, 3I) was likely located between rhombomere(s) 3 and/or 5 (data not shown), whereas the anterior border of the strong posterior broad band of *rarab* expression (open black arrowhead in Fig. 3H, 3I, 5E, 5F) was located at the posterior border of rhombomere 5 or perhaps within rhombomere 5 (Fig. 5E, 5F). We observed additional *rarab* expression in tissue lateral to the head which persisted until at least 12 hpf (data not shown). Strong *rarab* expression also occurred in the posterior neural plate, in the tail bud and adjacent mesoderm (Fig. 3H). Like *raraa*, expression of *rarab* was absent from the notochord (Fig. 3I).

During somitogenesis (12 hpf), the expression of *rarab* in the head and tail remained the same as that observed in earlier segmentation stages (Fig. 4F). Comparison of *rarab* and *raraa* expression patterns in the presumptive spinal cord revealed that *rarab* expression was distributed throughout the spinal cord, whereas *raraa* expression was graded along the anterioposterior axis.

At 24 hpf, a low level of *rarab* transcripts appeared ubiquitously distributed. Stronger expression of *rarab* occurred in the eyes, hindbrain and throughout the spinal cord.

Transcripts from *rarab* were detected in a cluster of cells within the dorsal diencephalon (data not shown). In the hindbrain, *rarab* at 24 hpf exhibited only a single band of expression in contrast to the multiple bands observed earlier. Using *egr2b* mRNA expression and the otic vesicle as positional markers, we located the anterior border of *rarab* expression in the hindbrain (black arrowhead in Fig. 5G, 5H) between rhombomeres 3 and 4 (Fig. 5G, 5H). Expression of *rarab* was also observed in non-neural tissues, including the ventral endodermal and mesodermal derivatives such as the pharyngeal endoderm, mesenchyme and tailbud (4G, 4H).

At 48 hpf, *rarab* expression was maintained in the hindbrain, eyes and diencephalon. Neuronal expression of *rarab* had expanded to more anterior brain regions with faint expression domains in the forebrain and midbrain. Expression of *rarab* was now prominent in the tectum (Fig. 4I, 4J) but had become diffuse in the hindbrain. In the pharyngeal region, *rarab* expression was still present (Fig. 4I). We found additional expression in two patches in ventral and lateral positions posterior to the otic vesicle, extending into the trunk region (4I, inset). We also detected expression in the pectoral fin bud (Fig. 4J).

Striped hindbrain expression of *rarab* faded and became diffuse during development, whereas *raraa* hindbrain expression continued in a strong band until at least 48 hpf. Earlier, at 11 hpf, both *raraa* and *rarab* were expressed in prominent bands with well-defined borders in the hindbrain. Within the posterior hindbrain, *rarab* transcripts appeared to be located more anteriorly than *raraa* transcripts. The anterior border of the broad band of *raraa* expression (open black arrowhead in Fig. 4E, 4F, 5A; 5B) lay within rhombomere(s) 6 and/or 7 while the anterior border of the two broad bands of *rarab* expression lay between

rhombomeres 3 and 5 (black arrowhead in Fig. 3H, 3I, 5G, 5H) and around rhombomere 5 (open black arrowhead in Fig. 3H, 3I, 5E, 5F). By 24 hpf the two broad bands of *rarab* expression fused into a single band of expression whose anterior border lay within rhombomeres 3 or 4 (Fig. 5H), while expression of *raraa* in the hindbrain remained striped until at least 48 hpf.

1.2.4. *rarg* expression

At 9 hpf, *rarg* mRNA expression in the epiblast was ubiquitous and extended to the marginal region (Fig. 3J), a pattern which differed from the more dorsally-restricted *raraa* and *rarab* expression patterns. Similarly, *RARG/Rarg* is the *RAR/Rar* predominately expressed in human and mouse skin (Krust et al., 1989). At about 10 hpf, *rarg* expression was limited to the anterior and posterior regions of the embryo. Unlike *raraa* and *rarab*, *rarg* was not expressed in the presumptive hindbrain at bud stage; instead anteriorly, *rarg* expression was limited to mesoderm adjacent to the head (Fig. 3K, 3L). Mouse *Rarg* transcripts are also expressed in mesoderm during late gastrulation (Ruberte et al., 1990). At 12 hpf, the head and tail expression persisted, but expression in the head was now restricted to two stripes parallel to the anterioposterior axis adjacent to the hindbrain (Fig. 4K). Joore et al. (1994) describes the striped staining as *rarg* expression in the anterior lateral mesenchyme. One-color-double in situ hybridization experiments with *egr2b* revealed that the anterior lateral mesenchyme stripes (Joore et al., 1994) described above are located in mesoderm flanking rhombomeres 3 and 5 (data not shown).

At 24 hpf, we began to detect *rarg* transcripts in the hindbrain, neural crest cells (Fig 4L, 4M; see also Joore et al., 1994), and in the tail. Within head mesenchyme, *rarg* expression occurred in neural crest-derived mesenchyme that will occupy the anterior

pharyngeal pouches (Fig. 4M; compare to *dlx2* expression, Akimenko et al., 1994). All three neural crest streams expressed *rarg*, whereas only posterior neural crest populations expressed *raraa*. Transcripts of *rarg* were not detected in the spinal cord (Fig. 4L). Non-neural *rarg* expression appeared diffuse.

At 48 hpf, hindbrain expression increased and showed sharp borders within the hindbrain, anteriorly at rhombomere 3 and posteriorly at the hindbrain/spinal cord border (Fig. 4N, 5J). In addition, a defined stripe appeared in the more anterior hindbrain, leaving a one-rhombomere-wide gap between the cerebellum and rhombomere 3 (Fig. 4N, 5J). In the dorsal hindbrain, *rarg* was expressed in narrow stripes at intervals one rhombomere wide (Fig. 5J), suggesting expression was located at rhombomere boundaries. Head expression of *rarg* at 48 hpf was more similar to *raraa* expression which is limited to the hindbrain, than *rarab* expression which was located in anterior brain regions, in clusters in the forebrain and the midbrain- hindbrain domain. We found prominent *rarg* expression in pharyngeal arches 1 and 2, in the more posterior arches, arches 3 to 7, and in the anterior neurocranium (Fig. 5I). Expression in the anterior pharyngeal arches was unique to *rarg*; *raraa* and *rarab* expression appeared in more posterior branchial regions. In addition at 48 hpf, expression of both *raraa* (Fig. 4D, 4E) and *rarab* (Fig. 4I, 4J) in the pharyngeal region was restricted to a lateral and ventral region bounded by the otic vesicle and the segmented mesoderm, whereas expression of *rarg* (Fig. 4N, 4O) in the anterior pharyngeal region was widely distributed. We also detected *rarg* expression in cells, probably mesenchymal cells, separating the eyes and forebrain (grey arrowhead in Fig. 4N) and in the pectoral fin buds (Fig. 4N, 4O). Although *raraa* and *rarab* are more closely related phylogenetically, expression of *rars* in the fin and tail bud is more similar between *rarg* and *rarab* than *raraa* and *rarab*. Tailbud expression of *rarg* was still visible at 48 hpf (Fig. 5K-M), in contrast to tailbud expression of *raraa* which was

absent by 24 hpf (Fig. 4B) and expression of *rarab*, which was lost from the tailbud after 24 hpf (data not shown).

1.3. Conclusions

In general, *rar* expression patterns coincide with the mRNA expression patterns of genes involved in the synthesis, transport, and degradation of RA, including *retinaldehyde dehydrogenase 2 (raldh2)*, *cellular retinoic acid-binding protein 2 (crabp2s)* and *cyp26*. In particular, expression of *raraa* (Fig. 4E, 4F) and *rarab* (Fig. 4H, 4I) in the paraxial mesoderm overlaps with *raldh2* expression (Grandel et al., 2002) and *crabp2a* and *crabp2b* expression (Sharma et al., 2005) at 11 hpf. During segmentation, expression of *cyp26b1*, which encodes the retinoic acid degrading enzyme Cyp26b1, overlaps *raraa* and *rarab* in the hindbrain (Zhao et al., 2005). Later, at 48 hpf, *rarg* and *cyp26b1* hindbrain expression overlap instead (Zhao et al., 2005). It may seem curious that the RA-degrading enzyme and RA receptor proteins are expressed at the same time and place. This coexpression may reflect the fine regulation of RA signaling in the developing embryo. These studies of the syntenic and phylogenetic relationships between zebrafish and human *RAR* genes, as well as the early expression patterns of the zebrafish genes, will provide the basis for future studies of *rar* gene function during development.

2. Experimental procedures

2.1. Cloning of *rar* genes

Clones of *raraa* and *rarab* were donated by P. Kushner and S. E. Stachel. We cloned a 486-basepair fragment of *rarg* (Accession number: S74156) using the following primers:

5'-CACCCGCCCTGCTCACGA-3' and 5'-
GAACCCGTTGAAAGTACACTGTTAAAAG-3'.

2.2. Whole mount in situ hybridization

Zebrafish embryos (AB strain) were raised as described by Westerfield (1995) and staged by hours post fertilization (hpf) at 28.5°C according to Kimmel et al. (1995). To prevent pigment formation, embryos were treated with 0.003% 1-phenyl-2-thiourea (PTU) in embryo medium at 12 hpf.

RNA in situ hybridization was carried out according to standard protocols described in Hauptmann and Gerster (1994). The following RNA probes were used: *krox20* (Oxtoby and Jowett, 1993; renamed *early growth response 2b (egr2b)*, refer also to ZFIN (see <http://zfin.org/cgi-bin/webdriver?Mlval=aa-markerview.apg&OID=ZDB-GENE-980526-283>; Sprague et al., 2002), *raraa* (Accession number: L03398; also referred to as *rara* by Joore et al., 1994), *rarab* (Accession number: L03399) and *rarg* (Accession number: S74156; also referred to as *rary* by Joore et al., 1994). Embryos were viewed with Leica MZ6 or MZ9 stereomicroscopes or with a Zeiss Axioplan microscope, and were photographed using a Nikon Coolpix 990 or 995 digital camera.

2.3. Sources of additional gene expression data

Some expression data for zebrafish genes cited here were retrieved from the Zebrafish Information Network (ZFIN), the Zebrafish International Resource Center, University of Oregon, Eugene, OR 97403-5274; World Wide Web (URL: <http://zfin.org/>), August, 2005 and NCBI Entrez Gene (Zhang et al., 2005; World Wide Web (URL: <http://www.ncbi.nlm.nih.gov/entrez/query.fcgi?db=gene>).

Some mouse gene expression data cited in this paper were retrieved from the Gene Expression Database (GXD), Mouse Genome Informatics Web Site, The Jackson Laboratory, Bar Harbor, Maine. World Wide Web (URL: <http://www.informatics.jax.org>), August, 2005.

Some human gene expression data cited in this paper were retrieved from The Human Genome Organisation (HUGO), London. World Wide Web (URL: <http://www.gene.ucl.ac.uk/nomenclature/index.html>), September, 2005.

CHAPTER III

**CHARACTERIZATION OF RETINOID-X RECEPTOR GENES *RXRA*, *RXRBA*,
RXRBB AND *RXRG* DURING ZEBRAFISH DEVELOPMENT**

The work described in this chapter was previously published in “Gene Expression Patterns,” Vol. 6. I share first authorship with A. Tallafuss. We were responsible for the majority of data collection, data analysis and writing. A. Tallafuss cloned *rxrg*. Y.L. Yan and L. Dudley cloned *rxra*, *rxrba*, and *rxrbb*. J.H. Postlethwait completed the syntenic analysis and contributed to writing. J.S. Eisen also contributed to writing.

1. Results and discussion

Retinoic acid (RA) signaling has been implicated in a variety of developmental processes including patterning of the central nervous system (CNS), paired appendages and other organs (Gavalas and Krumlauf, 2000; Grandel et al., 2002; Jiang et al., 2002). RA acts by binding to heterodimeric receptors composed of a retinoic acid receptor (Rar) and a retinoid-X receptor (Rxr); these receptors bind to retinoic acid response elements (RAREs) and modulate transcription of target genes [reviewed by (Bastien and Rochette-Egly, 2004)]. Rxrs also form heterodimers with other nuclear receptors, including thyroid-hormone receptors (TRs), peroxisome proliferator-activated receptors (PPARs), Vitamin D receptor (VDR), and liver X receptor (LXR) (Umesono and Evans, 1989; Willy and Mangelsdorf, 1999), indicating Rxrs mediate expression of a large variety of hormone-responsive genes. Malfunction of RA receptors has been linked to several cancers (Li et al. 1998; Soprano et al., 2004). Currently, RA and its analogs are under investigation as chemopreventative

agents in cancer therapy (Okuno et al., 2004) and Rxrs as potential targets for cancer chemotherapies (Crowe et al., 2004).

In this paper, we focus on retinoid-X receptors in zebrafish, a model for molecular and genetic studies of vertebrate development. Previous studies of *rxr* transcript accumulation during zebrafish development have provided a foundation for understanding when and where these genes function (White et al., 1994; Jones et al., 1995; Thisse et al., 2004; Kawakami et al., 2005), but knowledge of expression during more developmental stages is needed and a stronger comparison of various receptor expression patterns is necessary for a complete understanding of *rxr* gene expression.

Incomplete knowledge of gene expression patterns, in addition to recent availability of genomic information, prompted us to revisit the expression of *rxr* genes in concert with understanding their phylogenetic relationships to human orthologs. Based on conserved synteny between zebrafish and human chromosomes, we show that some of the zebrafish *rxr* genes were previously assigned inappropriate orthologies, and thus incorrect names. We provide detailed information about the phylogenies of the four known zebrafish *rxr* genes as well as more detailed descriptions of their expression patterns. This information is crucial for future studies of the functions of *rxr* genes during development and for understanding how malfunction of these genes may contribute to diseases such as cancer (Okuno et al., 2004).

1.1. Orthologies of zebrafish *rxr* genes

To properly compare expression dynamics among species, it is essential to evaluate orthologous genes. Two types of data help establish orthologies: phylogenetic analysis and conserved synteny.

Phylogenetic analysis of amino acid sequences rooted on related genes from protostomes and non-vertebrate chordates revealed three clades of vertebrate *Rxr* genes that arose after the divergence of vertebrate and non-vertebrate chordate lineages (Fig. 1). These relationships are consistent with the explanation that these genes appeared in the genome amplification events around the origin of vertebrates (Holland and Garcia-Fernandez, 1994). Our data suggest that *rxra* (AAH59576; Strausberg et al., 2002) and *rxrg* (Accession number NP_571228; Jones et al., 1995) are incorrectly named in the literature. Our results showed that the zebrafish gene formerly called *rxrg* (Accession number NP_571228; Jones et al., 1995) groups with high bootstrap support in the tetrapod *Rxra* clade, suggesting that NP_571228 is an ortholog of *Rxra*, rather than an ortholog of *Rxrg* as previously thought; thus, we have renamed NP_571228 as *rxra* (Table 1). Reciprocally, the gene previously named *rxra* (AAH59576; Strausberg et al., 2002) clusters with the tetrapod *Rxrg* clade, but with low bootstrap support, so additional data, described below, are required to confirm whether AAH59576 is the ortholog of *Rxrg*. Zebrafish have at least two additional *rxr* genes: *rxrb* (AAH54649, Strausberg et al., 2002) and *rxrd* (NP_571313, Jones et al., 1995). The tree shows with good bootstrap support that both genes are orthologs of *Rxrb* (Fig. 1), thus we have renamed them *rxrba* (formerly *rxrb*) and *rxrbb* (formerly *rxrd*; see also Table 1).

Human *RXRG* maps to Hosa1q24 (Fig. 2B1), and AAH59576 (formerly called *rxra* but which clusters with *Rxrg* in the phylogeny of Fig. 1) is on Zv5_scaffold1017 in the zebrafish genome. The orthologs of several genes located nearby in Zv5 are also located near *RXRG* in the human genome (Fig. 2B2 and 2B3). Furthermore, the orthologs of additional genes near *RXRG* in the central part of Hosa1q are located with AAH59576 on LG2 (Fig. 2B2-2B4). Of 165 protein-coding loci mapped to LG2 in the HS mapping panel (Woods et al., 2005), 22 have orthologs on Hosa1 (the location of *RXRG*), and none from Hosa9 (the

location of *RXRA*). Because analysis of conserved syntenies provides strong support for the orthology of AAH59576 to *RXRG* and corroborates the phylogenetic analysis, we have renamed this sequence *rxrg* rather than its previous name of *rxra*. The Zv5 assembly of the zebrafish genome shows the *rxrg* scaffold on LG20, but we mapped this sequence to LG2 (Postlethwait et al., 1998) and this location was later confirmed on four independent mapping panels (see <http://zfin.org/cgi-bin/webdriver?MIval=aa-markerview.apg&OID=ZDB-GENE-980526-36>), so it is likely that *rxrg* is assigned to the wrong linkage group in Zv5.

Table 1. Survey of recent and previous *Rxr* gene names.

Zebrafish Gene	Accession number	Previous Zebrafish Gene	Human Ortholog	Mouse ortholog
<i>rxra</i> *	<u>NP 571228</u>	<i>RXRγ</i> ¹ ; <i>rxrg</i> ³	<i>RXRA</i> ⁴	<i>Rxra</i> ⁵
<i>rxrba</i> *	<u>AAH54649</u>	<i>RXRβ</i> ¹ ; <i>rxrb</i> ^{2,3} ; <i>RXRε</i> ¹ ; <i>rxre</i> ³	<i>RXRB</i> ⁴	<i>Rxrb</i> ⁵
<i>rxrbb</i> *	<u>NP 571313</u>	<i>RXRδ</i> ¹ ; <i>rxrd</i> ³		
<i>rxrg</i> *	<u>AAH59576</u>	<i>RXRα</i> ¹ ; <i>rxra</i> ^{2,3}	<i>RXRG</i> ⁴	<i>Rxrg</i> ⁵

*this paper;

¹Jones et al., 1995;

²Strausberg et al., 2002;

³ZFIN (2003; <http://zfin.org/cgi-bin/webdriver?MIval=aa-pubview2.apg&OID=ZDB-PUB-030508-1>);

⁴HUGO (2005; <http://www.gene.ucl.ac.uk/nomenclature/index.html>);

⁵MGI (2005; <http://www.informatics.jax.org/>)

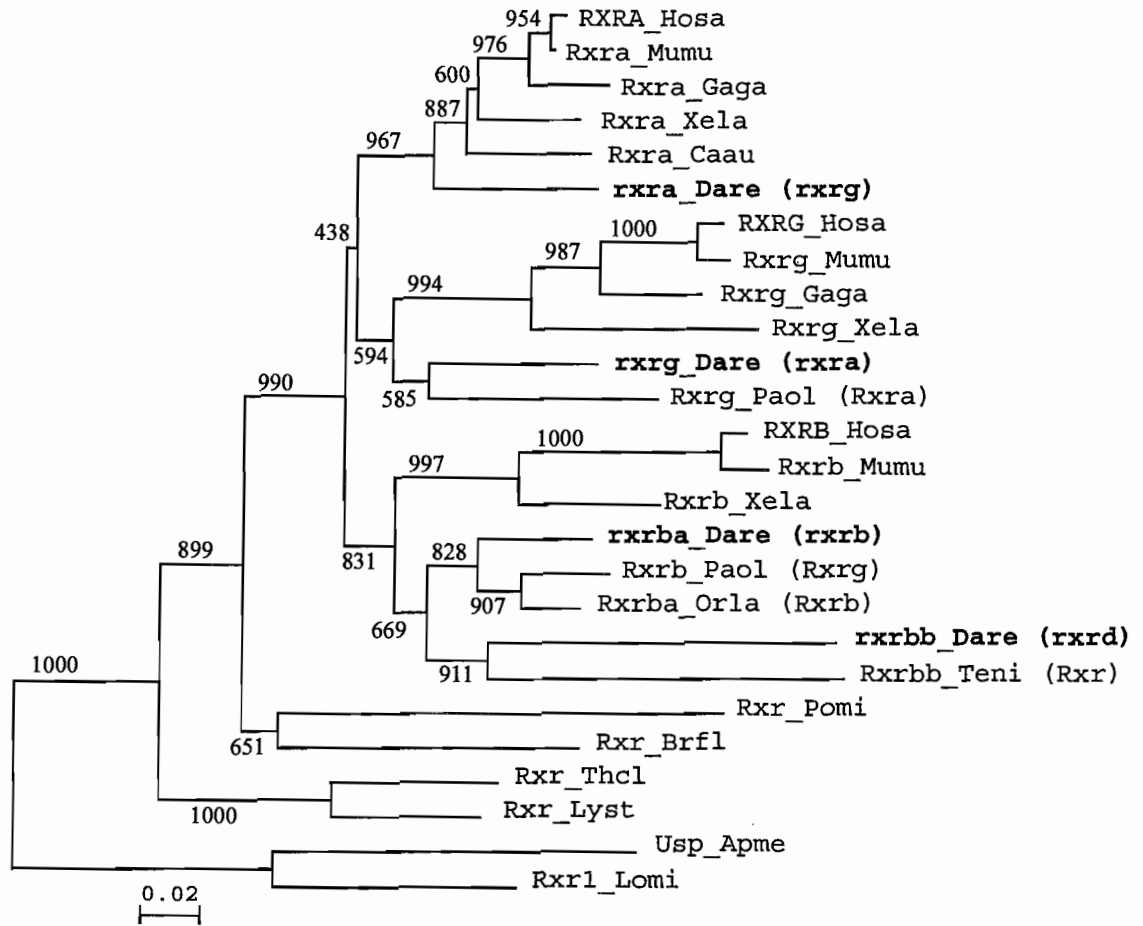


Fig. 1. Phylogenetic analysis of retinoid-X receptor proteins. Amino acid sequences were aligned by Clustal-X and trimmed to include unambiguously aligned regions; phylogenetic analysis used the neighbor-joining method (Saitou and Nei, 1987). Numbers at nodes are bootstrap values out of 1000 runs. Alignments are available on request. Species abbreviations: Apme, *Apis mellifera* (honey bee); Brfl, *Branchiostoma floridae* (amphioxus); (Caau, *Carassius auratus* (goldfish); Dare, *Danio rerio* (zebrafish); Gaga, *Gallus gallus* (chicken); Hosa, *Homo sapiens* (human); Lomi, *Locusta migratoria* (locust); Lyst, *Lymnaea stagnalis* (great pond snail); Mumu, *Mus musculus* (mouse); Orla, *Oryzias latipes* (medaka); Paol, *Paralichthys olivaceus* (flounder); Pomi, *Polyandrocarpa misakiensis* (an ascidian Urochordate); Teni, *Tetraodon nigroviridis* (pufferfish); Thcl, *Thais clavigera* (rock shell snail); Xela, *Xenopus laevis* (frog). Sequence accession numbers: RXRA Hosa AAH63827; Rxra Mumu NP_035435; Rxra Gaga XP_415426; Rxra Xela P51128; Rxra Caau AAO22211; rxra Dare NP_571228; RXRG Hosa NP_008848; Rxrg Mumu NP_033133; Rxrg Gaga NP_990625; Rxrg Xela P51129; Rxrg Dare AAH59576; Rxra Paol BAB71758; Hosa CAI95622; Rxrb Mumu NP_035436; Rxrb Xela AAH72132; Rxrb Dare AAH54649; Rxrg Paol BAB71759; Rxrb Orla BAD93255; rxrd Dare NP_571313; Rxr Teni CAG12025; Rxr Pomi BAA82618; Rxr Brfl AAM46151; Rxr Thcl AAU12572; Rxr Lyst AAW34268; Usp Apme NP_001011634; Rxr1 Lomi AAQ55293.

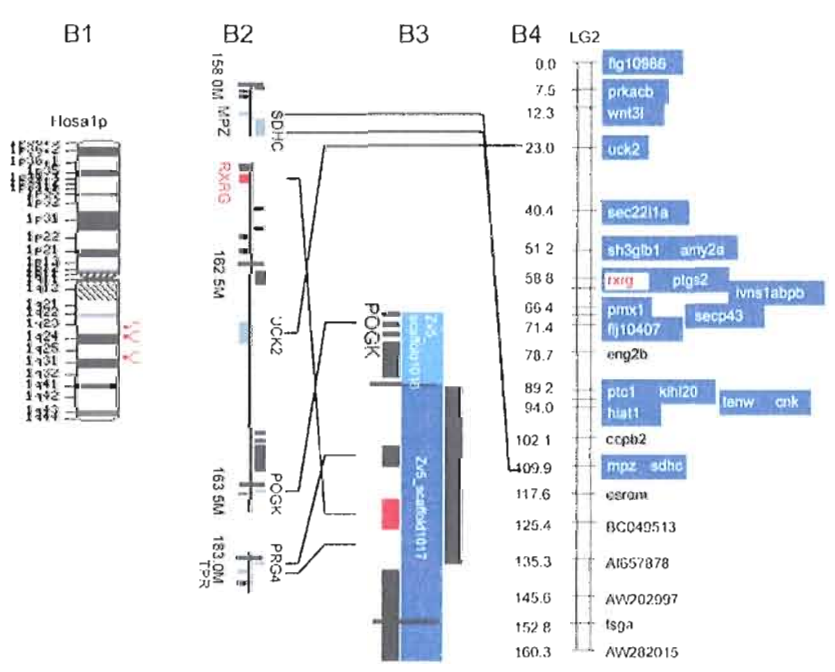
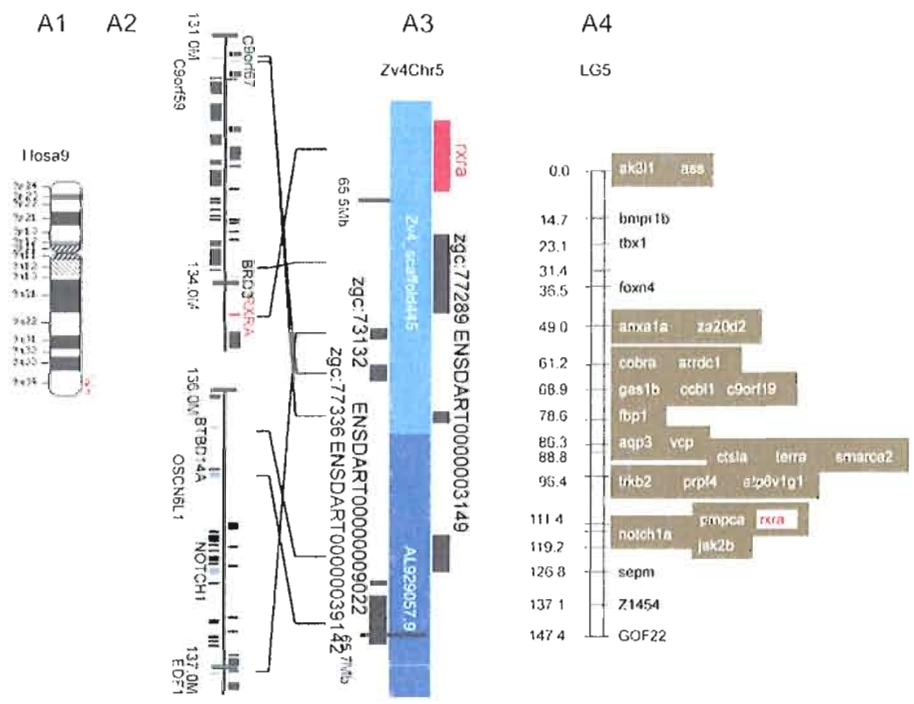
Phylogenetic analysis (Fig. 1) showed that *rxrba* and *rxrbb* are co-orthologs of *Rxrb*, but did not reveal whether they arose by a recent tandem duplication event or in the ancient teleost genome duplication (Amores et al., 1998; Postlethwait et al., 1998; Taylor et al., 2003). Analysis of conserved syntenies showed that *rxrba* and *rxrbb* are on LG19 and LG16, respectively (Fig. 3), which are duplicated chromosomes arising from the teleost genome duplication (Amores et al., 1998; Naruse et al., 2004; Woods et al., 2005).

In summary, analysis of phylogenies and conserved syntenies radically changes the nomenclature of zebrafish *rxr* genes (see also Table 2), with the old *rxrg* becoming *rxra*, the old *rxra* becoming *rxrg*, the old *rxrb* becoming *rxrba*, and the old *rxrd* becoming *rxrbb*. These revisions will help us to compare the expression patterns of these genes with their true orthologs in tetrapods.

1.2. Expression of *rxr* genes during zebrafish embryonic development

Having determined the orthologous relationships of zebrafish *rxr* genes, we next assayed their spatial and temporal expression patterns by whole mount RNA in situ hybridization during embryonic development. Although some aspects of *rxr* gene expression are available on ZFIN (<http://zfin.org/>; Sprague et al., 2001), current descriptions are incomplete and differ slightly from our results, discussed below. Our observations began in the cleavage period (0.75-2 hours post fertilization, hpf), extended through the blastula (2.25-4.66 hpf), gastrula (5.25-10 hpf), segmentation (10.33 -22 hpf), and pharyngula (24-42 hpf) periods, and concluded in the hatching period (48-72 hpf). Overall expression of *rxr* genes at representative time points is summarized in Fig. 4 and 5. Fig. 6 displays magnified views of *rxr* gene expression in specific tissues.

Fig. 2. Genomic analysis of conserved synteny for zebrafish *rxr* genes. A. *rxra* (NP_571228). A1 shows human chromosome 9 with regions relevant to zebrafish *rxra* expanded in A2. The location of human genes and gene names are from NCBI Map Viewer (http://www.ncbi.nlm.nih.gov/mapview/map_search.cgi?%20), with genes transcribed downwards shown on the right of the central line indicating the chromosome and genes transcribed upwards to the left of the line. A3 shows the *rxra*-containing region of the Zv4 zebrafish genome assembly (http://www.ensembl.org/Danio_rerio/), and A4 shows zebrafish linkage group 5 with loci orthologous to *Hosa9* genes shown in brown (Woods et al., 2000). B. *rxrg* (AAH59576). B1 shows *Hosa1*, and B2 shows relevant portions expanded. B3 is the portion of Zv5 containing *rxrg*, and B4 is LG2 with *Hosa1* orthologs shown in blue. C. *RXRβ* co-orthologs. C1 and C5 show the duplicated zebrafish linkage groups containing *rxrba* and *rxrbb*, with *Hosa6* orthologs indicated in yellow. C2 and C3 show the human chromosome and the region surrounding *RXRβ*. C4 shows the portion of Zv4 containing *rxrba*. The *rxrbb* sequence was not assembled in Zv4 or Zv5.



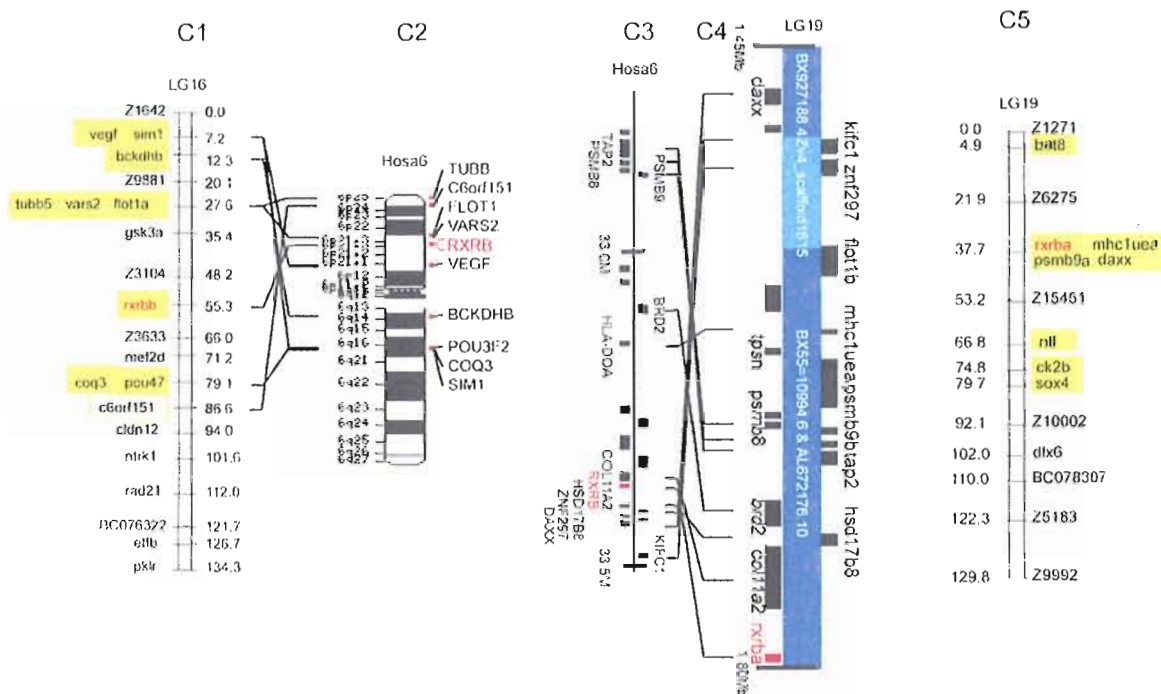


Fig. 3. Genomic analysis of conserved synteny for zebrafish *RXR*B co-orthologs. C1 and C5 show the duplicated zebrafish linkage groups containing *rxrba* and *rxrbb*, with *Hosa6* orthologs indicated in yellow. C2 and C3 show the human chromosome and the region surrounding *RXR*B. C4 shows the portion of *Zv4* containing *rxrba*. The *rxrbb* sequence was not assembled in *Zv4* or *Zv5*.

1.2.1. Maternal expression of *rxr* genes

Expression of mRNA transcripts of *Rxra*, *Rxrba*, *Rxrbb* and *Rxrg* was observed in early cleavage stages at 1.5 hpf (Fig. 4A), showing that these genes are maternally expressed. Cleavage and blastula period expression patterns of all four zebrafish *rxr* genes were similar, so Fig. 4A and 4B show only *rxrba* and *rxra* expression. We detected *rxra*, *rxrba*, *rxrbb* and *rxrg* transcripts from the blastula period through at least 48 hpf (Fig. 4), confirming previous results from Northern blots (Jones et al., 1995). During the blastula period, RNA in situ hybridization revealed that all *rxr* gene expression patterns are similarly uniform throughout the embryo. Distinctive *rxr* expression patterns arising during the gastrula period and

persisting through later developmental stages are described below. Expression patterns of *rxrba* and *rxrbb* were similar, so they are described in a single paragraph.

1.2.2. *rxra* expression

During mid-gastrulation (9hpf), *rxra* transcripts appeared throughout the embryo (Fig. 4C). Stronger expression was observed in the animal pole and to a lesser extent in the dorsal midline (data not shown). Between 10-11 hpf (late gastrulation), *rxra* expression remained ubiquitous (Fig. 4D, 4E). At 12 hpf, *rxra* was strongly expressed in the tail, but in the rest of the embryo, *rxra* expression was weak and ubiquitous (Fig. 5A).

At 24 hpf, faint *rxra* expression was found in the forebrain and eyes, and the pharyngeal endoderm (Fig. 5B, 5C); expression in tail mesoderm was also maintained (Fig. 5B). At later stages, expression remained in the eye and the pharyngeal endoderm, but was not detected in the brain (Fig. 6A).

At 48 hpf, anterior expression was limited to the ventral-most cell rows underlying the head (Fig. 5D). Additionally, *rxra* expression was detected medially within the mesoderm of the pectoral fin bud (Fig. 5E, 6B), placing *Rxra* in the appropriate position to transduce retinoic acid signaling for limb bud outgrowth (Stratford et al., 1996). Expression of *rxra* in the tail was maintained until at least 48 hpf (Fig. 6C). Currently, ZFIN has no RNA in situ hybridization data available for *rxra* (formerly *rxrg*).

1.2.3. *rxrba* and *rxrbb* expression

Despite significant differences in sequence, the spatiotemporal expression patterns of *rxrba* and *rxrbb* appeared similar. Weak expression, probably the result of low transcript levels, prevented detailed analysis, so we cannot exclude the possibility of subtle differences

in *rxrba* and *rxrbb* expression. Because *rxrba* and *rxrbb* expression patterns appeared similar, our description of *rxrbb* expression represents both *rxrba* and *rxrbb* expression. Spatially restricted *rxrbb* expression (formerly *rxrd*) has not been described in ZFIN (see <http://zfin.org/cgi-bin/webdriver?MIval=aa-fxfigureview.apg&OID=ZDB-FIG-050630-3780>), and there are no RNA in situ hybridization data available in ZFIN for *rxrba* (formerly *rxrb*).

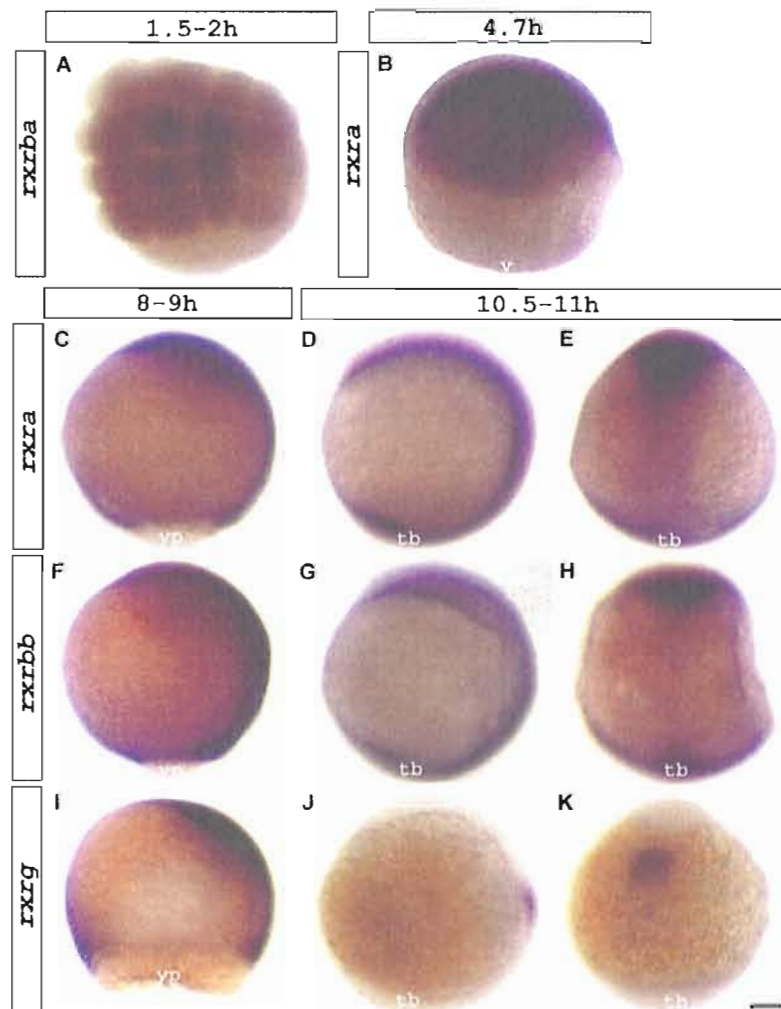


Fig. 4. Expression of *rxra* (B, C-E), *rxrba*, (A), *rxrbb* (F-H) and *rxrg* (I-K) visualized at 1.5-2 hpf (A), 4.7 hpf (B), 8-9 hpf (C,F,I) and 10.5-11 hpf (D,E,G,H,J,K). Dorsal view (A,E,H,K). Lateral view; anterior up and dorsal to the left (B,C,D,F,G,I,J). Abbreviations: v, vegetal pole; yp, yolk plug; tb, tailbud. Scale bar represents 93 μ m in A; 106 μ m in B, C-K.

During gastrulation, between 8-10.5 hpf, *rxrbb* expression remained ubiquitous (Fig. 4F). At 12 hpf, *rxrbb* (Fig. 5F) expression was similar to that in earlier periods but staining appeared fainter.

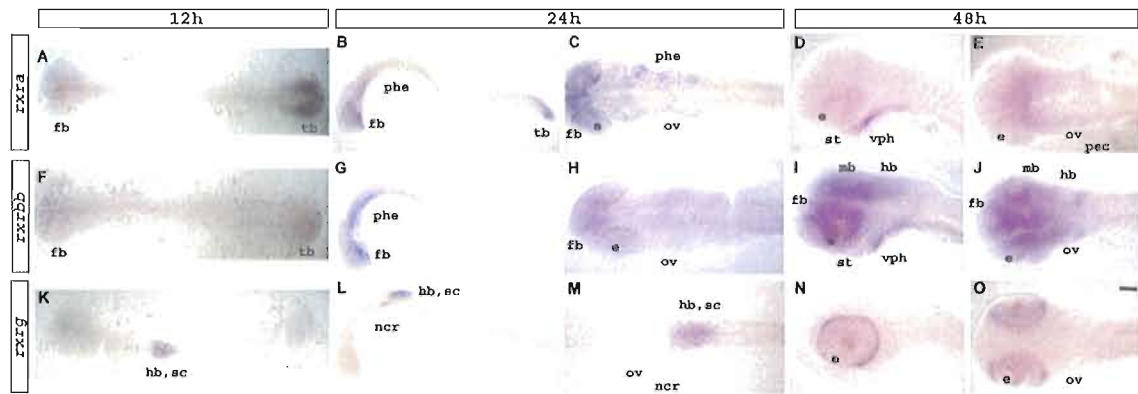


Fig. 5. Expression of *rxra* (A-E), *rxrbb* (F-J) and *rxrg* (K-O) at 12 hpf (A,F,K), 24 hpf (B,C,G,H,L,M) and 48 hpf (D,E,I,J,N,O). Refer to text for detailed descriptions. Flat-mount embryos seen from a dorsal view (A,C,E,F,H,J,K,M,O) or a lateral view (B,D,G,I,L,N). Anterior is to the left. Abbreviations: e, eye; fb, forebrain; hb, hindbrain; mb, midbrain; ncr, neural crest; phe, pharyngeal endoderm; ov, otic vesicle; sc, spinal cord; st, stomadeum; tb, tailbud; vph, ventral tissue in pharyngeal region. Scale bar represents 115 μ m in 4A,F,K; 100 μ m in 4B,G; 108 μ m in 4L; 40 μ m in 4C,M; 35 μ m in 4H; 32 μ m in 5D,E,I,J,N,O.

At 24 hpf, *rxrbb* expression became spatially restricted; in the neural tube, we detected expression mainly in the ventral diencephalon (Fig. 5G, 5H). We also detected expression in non-neural tissues: diffusely in pharyngeal endoderm and faintly in trunk and tail mesoderm (Fig. 5G, 5H). In the mesoderm, *rxrbb* expression occurred in the medial cell rows of each somite, along the dorsoventral axis (Fig. 6D, 6E). We describe these “somite stripes” of expression in this section as it was most evident in embryos stained for *rxrbb* expression (Fig. 5D, 5E), but weak expression in the medial somite stripes was evident for all *rxr* genes (data not shown). The timing and location of *rxr* expression in somites is interesting because it appears to be localized to the region traversed by motor axons, neural crest cells and sclerotome cells (Lewis and Eisen, 2004), suggesting that these receptors could be

involved in establishing or maintaining that pathway. At 48 hpf, *rxrba* and *rxrbb* were expressed in broad domains within the forebrain, eyes, midbrain and anterior hindbrain (Fig. 5I, 5J). Expression in the anterior endoderm described above was eventually restricted to the ventral-most cell layers (Fig. 6F).

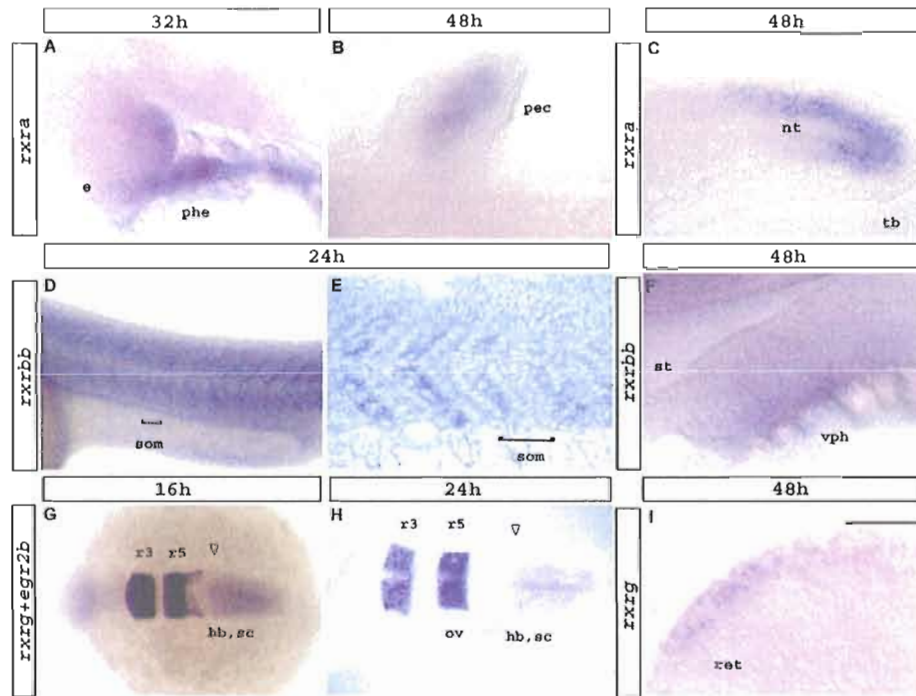


Fig. 6. Distinctive expression of *rxra* (A-C), *rxrbb* (F,G,H) and *rxrg* (D,E,I). Refer to text for detailed descriptions. Flat-mount embryos seen from a dorsal view (B,G,H) or a lateral view (A,C-F,I). Anterior is to the left. (A) Magnified view of *rxra* expression in the anterior endoderm and they eye at 32 hpf. (B) *rxra* pectoral fin bud expression at 48 hpf. (C) *rxra* tail expression at 48 hpf. (D,E) Stripes of *rxrbb* expression at 24 hpf in somites. Higher magnification view of somites. Bar in (D,E) marks the boundary from one somite to the next. (E) Sagittal section. (F) *rxrbb* expression in the ventral head tissue at 48 hpf. (G,H) Dorsal view of a whole-mount embryo. *rxrg* and *egr2b* expression at 16 hpf (G) and 24 hpf (H). Arrow in (G,H) marks anterior border of *rxrg* expression. (I) Magnified view of *rxrg* expression in the eye at 48 hpf. Abbreviations: e, eye; ov, otic vesicle; pec, pectoral fin bud; hb, hindbrain; nt, notochord; r3, rhombomere 3; r5, rhombomere 5; ret, retina; sc, spinal cord; st, stomadeum; tb, tailbud; vph, ventral tissue in pharyngeal region. Scale bar represents 60 μ m in 5A; 27 μ m in 5B; 63 μ m in 5C; 135 μ m in 5D; 48 μ m in 5E; 23 μ m in 5F; 159 μ m in 5G; 119 μ m in 5H; 19 μ m in 5I.

1.2.4. *rxrg* expression

In mid-gastrula stages, *rxrg* expression was uniform and broad (Fig. 4I), with additional intense expression in a region just posterior to the animal pole (data not shown), reminiscent of polster staining consistent with data available on ZFIN (<http://zfin.org/cgi-bin/webdriver?MIval=aa-imageview.apg&OID=ZDB-IMAGE-040908-344>). Beginning at 10 hpf, a definitive band of *rxrg* expression became evident in the presumptive posterior hindbrain and spinal cord along the dorsal surface (Fig. 4J, 4K). In late gastrula stages, *rxrg* exhibited specific expression in the presumptive hindbrain and spinal cord (Fig. 4I), but all other *rxr* genes were expressed ubiquitously (Fig. 4).

At 12 hpf, *rxrg* expression was restricted to the hindbrain as described for earlier stages (Fig. 5K). To confirm *rxrg* expression in the hindbrain during somitogenesis, we used *egr2b* (formerly *krox20*) as a marker for hindbrain rhombomeres (r), r3 and r5 (Oxtoby and Jowett, 1993), and performed double in situ hybridization experiments. In 16 hpf embryos, *rxrg* was expressed in the hindbrain, beginning within r7 and/or r8 and extending into the anterior spinal cord (Fig. 6G, 6H). Without the use of *egr2b*, however, in ZFIN, (see <http://zfin.org/cgi-bin/webdriver?MIval=aa-fxfigureview.apg&OID=ZDB-FIG-050630-2039>) the expression of *rxrg* in the neural tube was described as being localized to the spinal cord (beginning at 19 hpf).

During zebrafish development, *rxrg* expression in the posterior hindbrain and anterior spinal cord at 24 hpf was similar to that observed at earlier stages (Fig. 5L, 5M); this staining persisted until 42 hpf and finally faded at later stages (data not shown and Fig. 5N 5O; see also <http://zfin.org/cgi-bin/webdriver?MIval=aa-fxfigureview.apg&OID=ZDB-FIG-050630-15439>). In addition, at 24 hpf, *rxrg* was expressed in two patches in the lateral plate mesoderm flanking r6 (Fig. 4L, 4M). The position of these patches suggests that the

cells may be a part of the third stream of migrating neural crest cells. A similar expression domain of *rxrg* (see <http://zfin.org/cgi-bin/webdriver?MIval=aa-fxfigureview.apg&OID=ZDB-FIG-050630-12152>) was previously described as being located in pharyngeal arches 3-7. ZFIN (see <http://zfin.org/cgi-bin/webdriver?MIval=aa-fxfigureview.apg&OID=ZDB-FIG-050630-12152>) shows *rxrg* expression in the ventral part of the photoreceptor cell layer of the retina. We also detected *rxrg* transcripts in the retina beginning at 26 hpf.

At 48 hpf, *rxrg* was strongly expressed within the retina (Fig. 5N, 5O, 6I). During later stages (72 hpf), *rxrg* expression expanded throughout the eye (data not shown; see also Thisse et al., 2004); at 5 days post fertilization (dpf) *rxrg* was expressed in the entire photoreceptor layer of the retina (see also <http://zfin.org/cgi-bin/webdriver?MIval=aa-fxfigureview.apg&OID=ZDB-FIG-050630-3880>; Thisse et al., 2004). We failed to detect the faint *rxrg* expression previously described in the neural tube between 48 hpf and 5 dpf (see <http://zfin.org/cgi-bin/webdriver?MIval=aa-markerview.apg&OID=ZDB-CDNA-040425-772>). We were unable to detect some domains of low expression levels described by ZFIN, perhaps because we used a shorter probe (350 nucleotides (nt) for RNA in situ hybridization than the 1862 nt long fragment used by Thisse et al. (2004; see <http://zfin.org/cgi-bin/webdriver?MIval=aa-markerview.apg&OID=ZDB-CDNA-040425-772>), resulting in a weaker signal intensity.

1.2.5. Comparison of zebrafish *rxr* genes

During segmentation, we observed unique zebrafish *rxra* (12 hpf) and *rxrg* (10.3 hpf) expression patterns, whereas *rxrba* and *rxrbb* appeared similar and ubiquitously expressed until later stages. The early diffuse expression of *rxrba* and *rxrbb* became more restricted at 48

hpf; *rxrba* and *rxrbb* expression became localized to presumptive brain and pharyngeal regions. In contrast, *rxra* expression was regionally restricted during earlier stages. We observed *rxra* transcripts in tail mesoderm at 12 hpf. Additional later expression of *rxra* in the pharyngeal region appeared to coincide with *rxrba* and *rxrbb* pharyngeal expression (24 hpf). From 10.3 hpf onward the *rxrg* gene showed unique expression in the posterior hindbrain and anterior spinal cord as well as in the lateral mesoderm. Consistent with the dynamic temporal expression of other *rxr* genes, we observed *rxrg* transcripts in the retina, beginning at 26 hpf. The non-overlapping expression patterns of *rxra* and *rxrg* suggest that these genes do not directly interact but, rather that they have independent functions.

The expression domains of *rxrba* and *rxrbb* appear similar, consistent with the hypothesis that Rxrba and Rxrbb might have redundant functions. Diffuse expression, however, may have prevented us from detecting subtle variations that might indicate non-overlapping *rxrba* and *rxrbb* expression domains. The observation that retinoid receptors form homodimers and heterodimers with other nuclear receptors supports the idea of functional specificity conferred by a particular dimerizing partner. Zebrafish Rxrba and Rxrbb proteins may have different affinities for various binding partners, providing non-overlapping functions for the two genes despite overlapping expression patterns. Results in mouse, using different combinations of Rar/Rxr compound mutants suggested that Rars and Rxrs have preferred binding partners, but that Rar/Rxr proteins can substitute for each other (Kastner et al., 1997). This might explain how retinoid-X receptors, although broadly distributed, acquire functional specificity.

1.2.6. Comparison to *Rxr* gene expression in mouse and chick

A comparison of gene expression patterns among various vertebrates allows inferences regarding their evolution. Mouse *Rxra* and *Rxrb* are widely expressed (Mangelsdorf et al. 1992; Dolle et al., 1994) before they become restricted to the epidermis, squamous epithelia. In addition, gene expression was reported in intestine, bone, gonads, presumptive brain and spinal cord (Mangelsdorf et al., 1990; Ghose et al. 2004; see http://www.informatics.jax.org/searches/expression_report.cgi?_Marker_key=13294&returnType=assay%20results&order=printName). In chick, *Rxra* is also expressed in liver; in contrast to mouse, chick *Rxra* expression within the nervous system is restricted to neural crest and its derivatives (Rowe et al., 1991; Le Douarin and Smith, 1988). Because *Rxra* gene expression patterns are only partially maintained among vertebrates, their roles may have diverged in vertebrate evolution.

In early development, *rxrba* and *rxrbb* expression in zebrafish, like *Rxrb* expression in mouse, is mostly ubiquitous. Later, *rxrba* and *rxrbb* are expressed in the presumptive brain and in some non-neural tissues, and its mouse ortholog *Rxrb* is broadly expressed in the developing and adult central nervous system (Zetterstrom et al., 1999; see <http://www.informatics.jax.org/javawi2/servlet/WIFetch?page=markerDetail&key=13295>; Dolle et al., 1994). These comparisons suggest that zebrafish and mouse *Rxrb* orthologs might share conserved roles in the nervous system, but may play different roles in the development of non-neural structures. To date, *Rxrb* has not been reported in the chick genome.

In mouse and chick, *Rxrg* is expressed in skeletal muscle, the central nervous system, neural retina, and neural crest-derived elements of the peripheral nervous system (see <http://www.informatics.jax.org/javawi2/servlet/WIFetch?page=markerDetail&key=13296>)

(Mangelsdorf et al., 1992; Dolle et al., 1994; Georgiades et al., 1997), suggesting conserved roles for *Rxrg* among tetrapods. Most mouse and chick *Rxrg* expression domains overlap with zebrafish *rxrg* expression in the neural tube, neural crest, and retina. The similarity of *Rxrg* expression domains among zebrafish, mouse, and chick is not unexpected from our phylogenetic study, which grouped zebrafish *rxrg* (formerly *rxra*) in the tetrapod *Rxrg* clade. Despite many similarities of *Rxrg* expression patterns among various vertebrates, there are some species-specific differences. In zebrafish, *rxrg* expression is restricted to the posterior hindbrain and anterior spinal cord, whereas in mouse and chick, *Rxrg* transcripts are also detected in the forebrain, midbrain and anterior hindbrain (Hoover et al., 2000; Dolle et al., 1994). In the retina, *rxrg* in zebrafish is expressed probably in the photoreceptor cell layer (see also Thisse et al., 2004), and in the chick retina, *Rxrg* is expressed almost exclusively by photoreceptors, but in mouse retina, *Rxrg* is expressed by ganglion cells (Dolle et al., 1994) and in rat retina by amacrine cells, ganglion cells, and retinal progenitors (Kelley et al., 1995). In general, however, *Rxrg* expression patterns seem to be broadly maintained among vertebrates.

1.3. Conclusions

In this study, phylogenetic analysis and comparison of syntenic relationships provided assignments of zebrafish *rxr* genes to their tetrapod *Rxr* orthologs. This insight into the orthologous relationships of *rxrs* and *Rxrs* will enable us in future studies to better understand the function of *rxr* genes during development. Conserved *Rxr* gene expression domains among zebrafish, mouse and chick suggest that the *Rxr* family plays critical roles in diverse aspects of development. However, major differences in individual *Rxr* expression

domains suggest that Rxr functions may have diverged during the course of vertebrate evolution.

2. Experimental procedures

2.1. Cloning of *rxr* genes

We cloned partial fragments of the *rxr* genes (Table 2). Of note, a BLAST sequence alignment of our cloned *rxrba* and *rxrbb* sequences revealed no significant similarity between the two sequences, suggesting the similar expression patterns of *rxrba* and *rxrbb* were not the result of sequence similarities.

2.2. Whole mount RNA in situ hybridization

Zebrafish embryos (AB strain) were raised as described by Westerfield (1995) and staged by hours post fertilization (hpf) at 28.5°C according to Kimmel et al. (1995). To prevent pigment formation, embryos were treated with 0.003% 1-phenyl-2-thiourea (PTU) in embryo medium at 12 hpf.

RNA in situ hybridization was carried out according to standard protocols described in Hauptmann and Gerster (1994). The following probes were used: *egr2b* (previously called *krox20*; Oxtoby and Jowett, 1993), *rxra* (Accession number: NP_571228), *rxrba* (Accession number: AAH54649), *rxrbb* (Accession number: NP_571313), and *rxrg* (Accession number: AAH59576). To detect weak *rxr* gene expression in the trunk, we prolonged the incubation time in NBT/BCIP solution. Embryos were viewed with Leica MZ6 or MZ9 stereomicroscopes or with a Zeiss Axioplan microscope, and were photographed using a Nikon Coolpix 990 or 995 digital camera.

Table 2. Primer sequences used to obtain *rxr* clones.

Gene	Accession Number	Primer Sequences	Size of clone	Previous gene name ZFIN-ID * NCBI Entrez ID**
<i>rxra</i>	<u>U29894</u>	5'-GCCAACCTGAGCCCGTCTG-3' and 5'- GTTCCCTTAATGCCTCACCTCTGAT- 3'	430 nt	<i>rxrg</i> *ZDB-GENE-990415- 243 **30389
<i>rxrba</i>	<u>U29942</u>	5'- ACTCTGGGGCTTTACTGTGTCTCA-3' and 5'-AACCCCGGCCTGCATTCATA-3'	628 nt	<i>rxrb</i> (formerly <i>rxre</i>) *ZDB-GENE-980526- 436 **30530
<i>rxrbb</i>	<u>U29941</u>	5'- AATCGTTGCCAGTACTGCCGCTATC- 3' and 5'- ATCTCCCAATTTTCCTCTGACGCAAC TA-3'	877 nt	<i>rxrd</i> *ZDB-GENE-990415- 242 **30486
<i>rxrg</i>	<u>U29940</u>	5'-ATAGACACTTTCCTCATGGAG-3' and 5'-AAACTGATTGCTGGTACTG-3'	349 nt	<i>rxra</i> *ZDB-GENE-980526- 36 **30464

*[http://zfin.org/cgi-bin/webdriver?MIval=aa
accessionselect.apg&select_from=ACCESSION;](http://zfin.org/cgi-bin/webdriver?MIval=aa%0D%0Aaccessionselect.apg&select_from=ACCESSION;)

**<http://www.ncbi.nlm.nih.gov/entrez/query.fcgi?CMD=search&DB=gene>

2.3. Sources of additional gene expression data

Gene expression data for this paper were retrieved from the Zebrafish Information Network (ZFIN), the Zebrafish International Resource Center, University of Oregon, Eugene, OR 97403-5274; World Wide Web (URL: <http://zfin.org/>), August, 2005 and NCBI Entrez Gene (Zhang et al., 2005; World Wide Web (URL: <http://www.ncbi.nlm.nih.gov/entrez/query.fcgi?db=gene>).

Some mouse gene expression data for this paper were retrieved from the Gene Expression Database (GXD), Mouse Genome Informatics Web Site, The Jackson Laboratory, Bar Harbor, Maine. World Wide Web (URL: <http://www.informatics.jax.org>), August, 2005.

Some human gene expression data for this paper were retrieved from The Human Genome Organisation (HUGO), London. World Wide Web (URL: <http://www.gene.ucl.ac.uk/nomenclature/index.html>), September, 2005.

CHAPTER IV
NETRIN SIGNALING IS REQUIRED FOR DEVELOPMENT OF AN IDENTIFIED
ZEBRAFISH MOTONEURON

Summary

Here we show that two initially equivalent zebrafish motoneurons, CaP and VaP, respond differently to the same axon guidance molecule. CaPs extend axons that pause at several intermediate targets as they navigate toward their ventral muscle targets. Different Netrins are expressed by different intermediate targets, suggesting a molecular mechanism for motoneuron axon outgrowth. VaPs extend short axons that stop at the first defined intermediate target, the muscle pioneers. Previous work showed that both CaP and muscle pioneers are required for VaP formation. We show, by morpholino mediated gene knockdown, that Netrins are unnecessary for normal CaP axon extension, but that they are necessary to prevent the VaP axon from extending to the CaP axon's targets. We also identify Deleted in colorectal carcinoma as a Netrin receptor that mediates Netrin's ability to cause VaP axons to stop at muscle pioneers. Collectively, our results suggest Netrins do not function as long-range cues to guide motoneuron axons, rather they function locally to restrict axon outgrowth.

Introduction

Distinct motoneurons innervate different muscles enabling coordinated movements; improper motor development can affect behavior. Zebrafish primary motoneurons are an excellent system in which to study the mechanisms underlying motoneuron development.

Individual primary motoneurons are distinguished by their rostrocaudal positions within the spinal cord and their axonal trajectories (Eisen et al., 1986; Myers et al., 1986). Such features enable us to analyze the development of neural connectivity at the level of individual neurons and their respective targets. In particular, we study caudal primary motoneuron (CaP) and variable primary motoneuron (VaP) development to find genes involved in establishing cell appropriate axon morphology. CaP is present in all spinal hemisegments and extends a long axon into ventral muscle. CaP axon outgrowth follows a stereotyped path and includes pausing at several intermediate targets (Beattie et al., 2000; Melançon et al., 1997) before reaching its final target, ventrolateral axial muscle (Myers et al., 1986). Within a trunk hemisegment, CaP's axon exits the spinal cord at the ventral root and, by 18-19 hpf (Eisen et al., 1990), extends to the first intermediate target, the muscle pioneer cells that define the horizontal myoseptum (HM, Fig. 1A) (Beattie et al., 2000; Melançon et al., 1997), where it may pause for up to an hour (Eisen et al., 1986). By 20 hpf (Eisen et al., 1990), the CaP axon continues toward ventral muscle, typically pausing at two additional intermediate targets, a region adjacent to the ventral aspect of the notochord (VNC, Fig. 1A) and the ventral-most aspect of the ventral muscle (VM, Fig. 1A) (Beattie et al., 2000) before wrapping around the ventral aspect of the myotome and continuing dorsally along the lateral surface at the anterior boundary of the myotome (Myers et al., 1986). By contrast to CaP, VaP is present in only about half of the spinal hemisegments, is located rostrally or caudally to CaP, extends a short axon that remains stalled at the muscle pioneers, and typically dies by 36 hours postfertilization (hpf) (Eisen, 1992; Eisen et al., 1990).

CaP and VaP initially form an equivalence pair (Eisen, 1992). In a given spinal hemisegment containing a presumptive CaP and VaP pair, if the nascent CaP is ablated the

nascent VaP will develop as a CaP, extending a long axon into ventral muscle (Eisen, 1992). This work indicated that CaP is necessary for VaP formation. Additional experiments also demonstrated that muscle pioneers are necessary for VaP formation (Eisen and Melançon, 2001). In the absence of muscle pioneers, VaP axons extended beyond muscle pioneers and VaP essentially develops as a second CaP. However, the molecular mechanisms involved in distinguishing CaP and VaP have yet to be determined.

Netrins, secreted proteins with roles in axon guidance, vascular development, organogenesis, and cell survival [reviewed by (Rajasekharan and Kennedy, 2009)], may also be involved in CaP and VaP development. Mutant analysis in flies revealed that two Netrins that are expressed in muscle targets for motoneurons, NetrinA and NetrinB, are necessary for peripheral motoneuron axon outgrowth (Mitchell et al., 1996). Similarly, in zebrafish Netrins are expressed by muscle pioneers and by other intermediate targets of the CaP axon. This expression pattern raises the possibility that Netrins may be involved in guiding CaP and/or VaP axons to intermediate targets. Alternatively, rather than functioning at a distance to guide motoneuron axons, Netrins may function as local guidance cues. Mouse Netrin-1 is expressed in intermediate targets for axons of retinal neurons and functions there to guide axons out of the immediate region; in the absence of Netrin-1 retinal neurons project aberrantly into neighboring tissue (Deiner et al., 1997). Recent examination of distribution of Netrin proteins in embryonic chick spinal cord using Netrin-specific antibodies revealed that Netrins may function locally or from afar to guide commissural axons to the floorplate (Kennedy et al., 2006). Generating anti-Netrin and anti-Dcc antibodies against zebrafish Netrins and Dcc will provide important tools to analyze Netrin signaling in spinal motoneuron development. Here we examine possible roles for Netrins in CaP and VaP development.

Materials and Methods

Animal husbandry and lines

Zebrafish embryos were obtained from natural spawning of ABC wild-type, *parg^{mn2Et}* (Balciunas et al., 2004), or *Tg(mnx1:GFP)ml2* (Flanagan-Steet et al., 2005) transgenic lines. Fish were staged by hours postfertilization at 28.5°C (Kimmel et al., 1995).

RNA in situ hybridization

RNA in situ hybridization using antisense-digoxigenin labeled *deleted in colorectal carcinoma (dcc)* (Fricke and Chien, 2005), *neogenin 1 (neo1)* (Mawdsley et al., 2004), *neogenin 2 (neo2)*, and *uncoordinated 5b (unc5b)* (Lu et al., 2004) oligonucleotide probes was carried out according to protocols described in Appel and Eisen (1998). Fluorescent in situ hybridization using *netrin 1a (ntn1a)* (Lauderdale et al., 1997), *netrin 1b (ntn1b)* (Strahle et al., 1997) and *netrin 2 (ntn2)* (Park et al., 2005) antisense probes was performed as described by Welten et al. (2006) with the following modifications provided by J. Talbot (personal communication): probes against *ntn1a* mRNA were made with dinitrophenyl (DNP) labeled nucleotides (PerkinElmer Life and Analytical Sciences, Inc., Shelton, CT, USA). Anti-DNP-HRP conjugated antibody and subsequent development with the TSA/Cy5 fluorescent system (PerkinElmer Life and Analytical Sciences, Inc., Shelton, CT, USA) was used to visualize mRNA expression.

Immunohistochemistry

The following primary antibodies (Abs) were used: monoclonal mouse zn1 (Trevarrow et al., 1990), monoclonal mouse znp1 (Trevarrow et al., 1990), monoclonal mouse F59 (Crow and Stockdale, 1986), and JL-8 monoclonal mouse anti-GFP (Clontech

Laboratories, Inc., Mountain View, CA, USA). The following secondary antibodies were used: goat anti-mouse Alexa-488 (Invitrogen-Molecular Probes; Eugene, OR, USA) and goat anti-mouse-HRP (The Jackson Laboratory, Bar Harbor, ME, USA).

Motoneuron cell bodies and axons were visualized with combined labeling using *zn1* and *znpl* (hereafter referred to as *zn1/znpl*) (Hutchinson et al., 2007) or with transgenic lines that express GFP in motoneurons, *Tg(mnx1:GFP)ml2* or *parg^{mn2Et}*. Slow muscle fibers, including muscle pioneers, were visualized by F59 antibody staining (1:10) using the antibody protocol described by Hutchinson et al. (2007). Anti-GFP antibody staining was used to visualize GFP expression in embryos that were first taken through the RNA in situ hybridization (ISH) protocol described above (Welten et al., 2006). Briefly, embryos were fixed after ISH for 1 hour in 4% PFA in 1x PBS at 4°C, washed for 30 minutes in PBST, incubated with primary antibody, JL-8 anti-GFP (1:200), and secondary antibody, goat anti-mouse-HRP (1:200), as described in Hutchinson et al. (2007). GFP expressing cells were visualized by diaminobenzidine (DAB) development as described in Appel and Eisen (1998).

Morpholinos

Morpholino sequences and reverse transcription PCR

The antisense oligonucleotide morpholinos (MOs) described in Table 1 were used to knock down zebrafish Netrins and Dcc or as controls to confirm MO specificity. All described MOs were designed by Gene Tools (Philomath, OR, USA). Reverse transcription (RT)-PCR was used to assay wild-type transcript knock down in splice-blocking MO-injected embryos. Table 1 lists primer pairs used to determine efficacy of MO knockdown. PCR conditions were as described in Suli et al. (2006).

Table 1. MO sequences used to knock down Netrins and Dcc and RT primer sequences used to confirm MO efficacy.

MO	MO Sequence (5'-3')	RT-PCR primers (5'-3')	Reference
<i>ntn1a</i> splice-blocking (SB) MO	ATGATGGACTTAC CGACACATTCGT	<i>ntn1a</i> pre-mRNA (F1 X R1) <i>ntn1a</i> mRNA (F1 X R2) F1: CTTTCGGAGACGAAAACGAG R1: GTAGGCGCTTTCCAGAGATG R2: CTTTGCAGTAGTGGCAGTGG	Suli et al. 2006
<i>ntn1a</i> 5-mispair MO	ATcATGcACTTAgC GACAgATTgGT (lower case letters represent mismatches)	n/a	n/a
<i>ntn1b</i> SBMO	TAGTTTAGAAATG ACTCACCGACAC	<i>ntn1b</i> pre-mRNA (F1 X R1) <i>ntn1b</i> mRNA (F1 X R2) F1: CCGACATCAAAGTGACCTTC R1: GAGCCATCCACACTTGTGTA R2: TGCACGTCGGTGTGATATAG	complementary to <i>ntn1b</i> exon 1/ intron 1- 2 boundary
<i>ntn2</i> SBMO	TTTCGTGACTTACG TAAGCACTCGT	net2E1F: TCCGGAGTGTGATCGATGTA net2E3R: CCTTTAGCACAGCGGTTACA	netrin2 SBMO3 (Suli, 2007)
<i>dcc</i> TBMO	GAATATCTCCAGT GACGCAGCCCAT	n/a	Suli et al., 2006
standard control MO	CCTCTTACCTCAGT TACAATTTATA	n/a	Gene Tools https://store2.gene-tools.com/node/7

Morpholino injections

The following amounts of MO diluted in 0.2% phenol red solution in water were injected in 1-2 cell stage embryos: standard control MO, 0.5-5.3 ng; *ntn1a* SBMO, 2.1-8.9 ng; *ntn1b* SBMO 5.6-15 ng, *ntn2* SBMO, 5.2-18 ng, and *dcc* TBMO, 0.5-5.2 ng. For double MO injections the same amount of MO was injected as individual MO experiments, but in combination. Injected amounts were calculated by measuring the diameter of a bolus injected into an oil droplet.

Single cell labeling

Individual primary motoneurons were labeled as previously described (Eisen and Melançon, 2001; Eisen et al. 1989) with the following modification: cells were injected with a 5% or 2.5% solution of either tetramethylrhodamine-dextran or Alexa Fluor®488-dextran (3000 MW, anionic; Invitrogen-Molecular Probes, Eugene, OR, USA) in 0.2M KCl. To avoid photodamaging dye-injected cells, they were allowed to recover for one hour in a dark, 28.5°C incubator before imaging, were imaged at only three time points over 12 hours, and were scanned for less than five minutes.

Microscopy

Images of fixed zebrafish embryos were captured on a Zeiss Axioplan equipped with a digital camera, or on a Zeiss Pascal confocal microscope. Images of living embryos were captured at 24, 30 and 36 hpf using a Zeiss Pascal confocal microscope with a 40x water immersion objective. The brightness and contrast of images was adjusted with Zeiss LSM Image Browser (Version 4.2.0.121, Carl Zeiss MicroImaging, Thornwood, NY, USA), or Photoshop CS4 Extended (Version 11.0, Adobe Systems, Inc., San Jose, CA, USA).

Antibody production

Polyclonal peptide antibodies against individual zebrafish Netrins were generated commercially by Alpha Diagnostic International (San Antonio, TX, USA). Rabbits were injected with peptides antigens conjugated to keyhole limpet hemocyanin (KLH) of the following sequences: Ntn1a, KGDERHRNCHTCDAS(P); Ntn1b, KGEERSRDCNICDAT(P) and, Ntn2, SLVERDDRPAVRTC. Resulting antisera in

concentrations ranging from 1:10 – 1:100 were screened on sectioned zebrafish embryos following methods in (Devoto et al., 1996).

Monoclonal antibodies against full length zebrafish Ntn1a, Ntn1b, Ntn2 and Dcc will be generated in collaboration with NeuroMAB (Davis, CA, USA). Mice will be injected with proteins derived from full length *ntn1a* (Lauderdale et al., 1997), *ntn1b* (Park et al., 2005), *ntn2* (Park et al., 2005), and *dcc* (A. Lim, unpublished) clones subcloned into protein overexpression vectors. Antisera will be screened in sectioned zebrafish embryos following methods in (Devoto et al., 1996).

Results

netrins are expressed by intermediate targets of the CaP axon

mRNAs encoding three zebrafish Netrins, Ntn1a, Ntn1b, and Ntn2, are expressed in or near the intermediate targets of CaP axons. At 15-16 hpf *ntn1a* mRNA is expressed by muscle pioneers (Lauderdale et al., 1997). Expression of *ntn1a* in muscle pioneers remains at 24 hpf (asterisks in Fig. 1C) and later (data not shown) (Suli, 2007) after CaP axons have extended beyond the region. At 18 hpf *ntn1b* mRNA is expressed in the hypochord (Strahle et al., 1997). Expression of *ntn1b* in the hypochord remains at 24 hpf (Fig. 1B, green) (Park et al., 2005), but by 36 hpf, expression is lost (Park et al., 2005; Strahle et al., 1997). Around 18 hpf, *ntn2* mRNA is expressed in adaxial cells (Park et al., 2005), the precursors of slow muscle (Devoto et al., 1996), and at 24 hpf *ntn2* mRNA is expressed in ventrolateral somite (Fig. 1B, purple) (Park et al., 2005). Thus, *netrins* are expressed at the appropriate times and places to function as signals for CaP and VaP axon outgrowth.

Because *ntn1a* is first expressed in the muscle pioneers at about the time they are contacted by CaP axons, we tested whether CaPs are necessary for *ntn1a* expression. We

manually removed CaPs, as well as other primary motoneurons, prior to axon outgrowth (Appel et al., 2001). *ntn1a* expression in the muscle pioneers was unaffected by the absence of motoneurons (data not shown), suggesting that *ntn1a* expression in muscle pioneers does not require contact by motor axons.

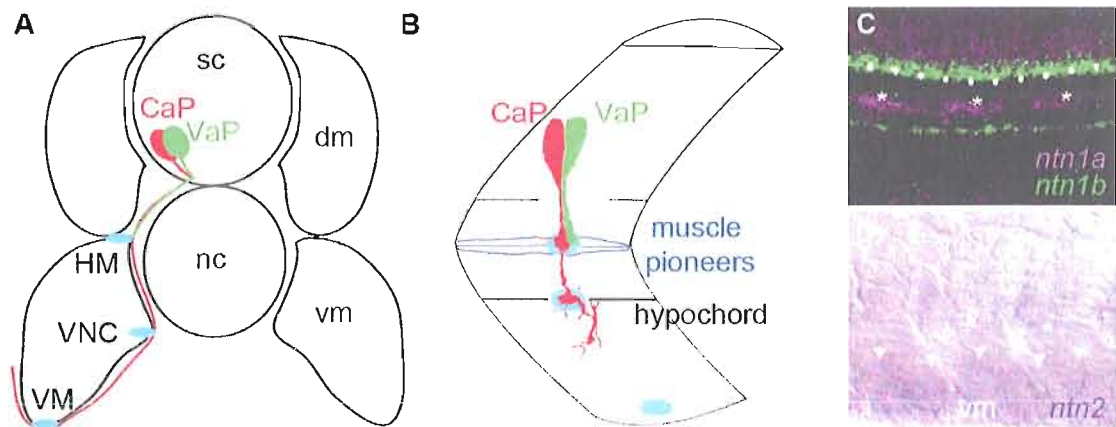
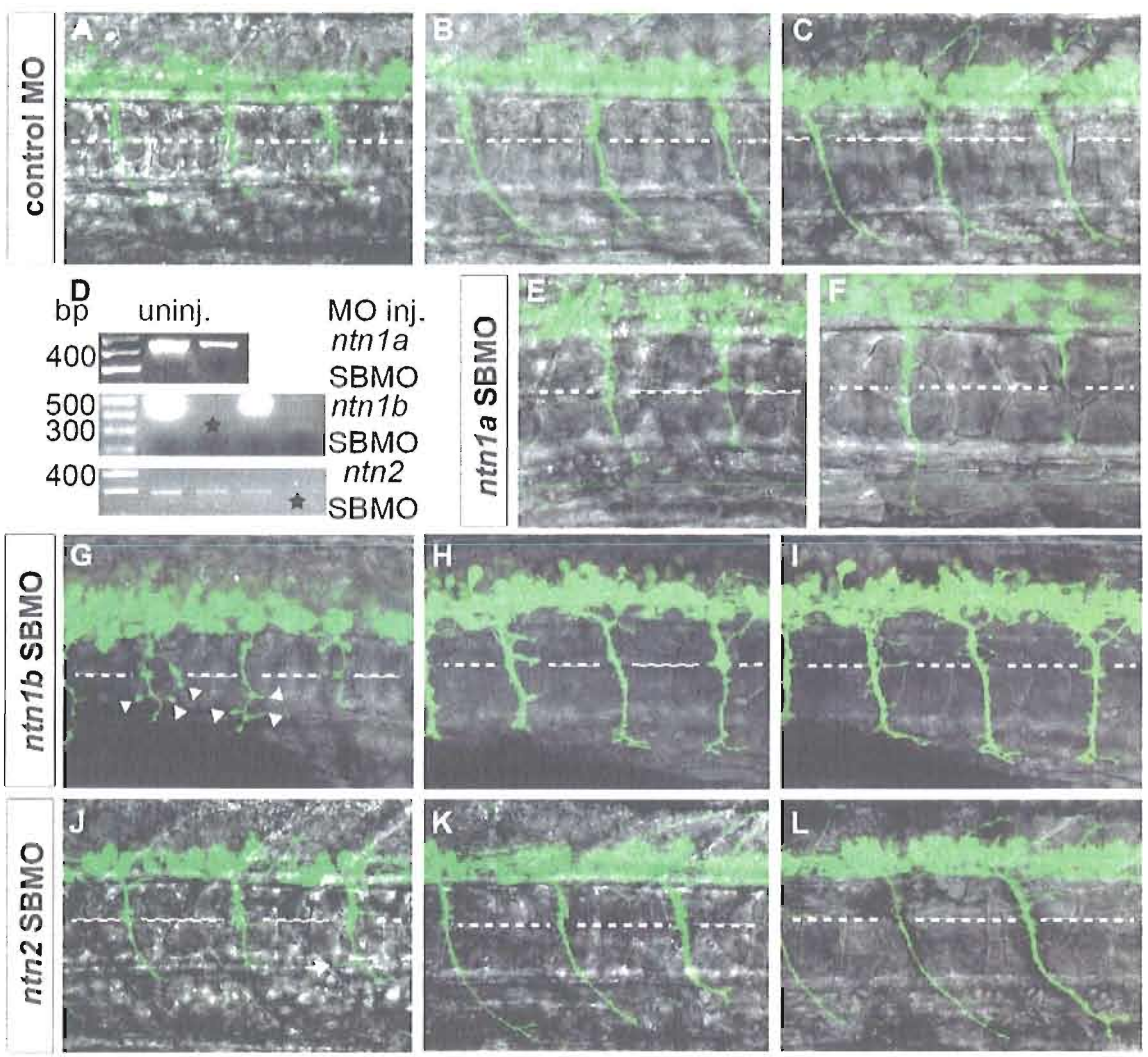


Fig. 1. Netrin mRNAs are expressed at intermediate targets for the CaP axon. A. Schematized view of a cross section through an embryonic zebrafish trunk showing CaP (red) and VaP (green) cell bodies in the sc and intermediate targets (blue ellipses) of the ventrally projecting axons. Both CaP and VaP project to HM. However, only the CaP axon continues towards the VNC and VM. B. Schematized view of one spinal hemisegment including sc and overlaying muscle. All subsequent images of CaP and VaP will be laterally oriented with anterior to the left, unless stated otherwise. Varicosities of CaP and VaP axons contacting muscle pioneers (blue) at the HM and later CaP axon varicosity at the level of the hypochord (solid black line) which is adjacent to the VNC target are emphasized. C. Confocal stack of *ntn1a* and *ntn1b* mRNA expression in zebrafish trunk at 24 hpf; *ntn1a* is expressed in spinal cord (purple) and muscle pioneers (purple and *). *ntn1a* staining was false colored purple. *ntn1b* mRNA (green) is expressed in floor plate (white dots) and hypochord, located ventrally to the floor plate. D. Brightfield image of lateral surface of zebrafish trunk at 24 hpf reveals *ntn2* is expressed in ventral somite (white arrowheads); asterisks denotes muscle pioneers, cells that do not express *ntn2*. Abbreviations: HM, horizontal myoseptum intermediate target; VNC, ventral aspect of notochord intermediate target; VM, ventral aspect of ventral muscle intermediate target; dm, dorsal muscle; nc, notochord; sc, spinal cord; vm, ventral muscle. These abbreviations will be used in all subsequent figures.

Netrins are unnecessary for CaP axon extension

Expression of Netrin mRNAs in CaP axon intermediate targets raised the possibility that Netrins might be required for normal CaP axon extension. To test whether Netrins are necessary for CaP axon extension, we knocked down Ntn1a, Ntn1b, and Ntn2 using MOs. When we injected a standard control MO, CaP axons exited the spinal cord and extended normally (Fig. 2A-C), as they did with *ntn1a* 5-mispair control MO (data not shown). Reducing wildtype *ntn1a* did not affect CaP axon extension into ventral muscle (Fig. 2D-F). By contrast, in the absence of Ntn1b, we observed some CaP axons with extra branches that strayed from their typical path (white arrowheads in Fig. 2G). However, by 30 hpf, a few CaPs had retracted the extra branches and all CaP axons had extended normally into ventral muscle (Fig. 2H). At 36 hpf, CaP axons in *ntn1b* MO-injected embryos had retracted more ectopic branches and began to extend along the lateral surface of the boundary between adjacent myotomes (Fig. 2I). At 24 hpf CaP axons formed some a few ectopic branches at the level of the hypochord when Ntn2 was absent (white arrowhead in Fig. 2J). However, by 30 and 36 hpf, CaP axons had retracted the ectopic branches and extended normal axons into ventrolateral muscle (Fig. 2K,L). Loss of Ntn1a had no effect on CaP axon extension and although loss of Ntn1b or Ntn2 resulted in early ectopic branching CaP axons began to establish their correct axon arbor by at least 30 hpf. Not all CaP axons in *ntn1b* and *ntn2* MO injected embryos produced ectopic branches. Careful cell counts will need to be performed to confirm these results. These results suggest that Netrins are unnecessary for CaP axons to extend to ventral muscle, but that Ntn1b and Ntn2 might play a role in preventing exuberant CaP axon branching.

Fig. 2. Netrins are unnecessary for CaP axons to extend into ventral muscle. A-C, E-L. Confocal stacks of GFP expressing motoneuron axons in living *Tg(mnx1:GFP)* embryos injected with various MOs. A-C. In standard control MO-injected embryos CaP axons extend to the VNC by 24 hpf (A), the VM by 30 hpf (B), and by 36 hpf have extended past the VM and are wrapping around the ventral aspect of the ventral myotome (C). D. RT-PCR results confirming uninjected embryos have wildtype *ntn1a* (450 bp band), *ntn1b* (500 bp band), or *ntn2* (300 bp band) transcript. Starred lanes show wildtype netrin transcripts are reduced or absent after injecting 0.9 ng of *ntn1a* SBMO, 8.0 ng of *ntn1b* SBMO, or 5.0 ng of *ntn2* SBMO. E-F. In *ntn1a* SBMO injected embryos CaP axons reach the VNC by 27 hpf (E) and the VM by 34 hpf (F). The CaP axon on the far right of F is not fragmented; this particular confocal stack lacks several slices containing the CaP axon. G-I. In *ntn1b* SBMO injected embryos CaP axons extend to VNC by 24 hpf (G). CaP axons in this particular embryo also extend ectopic branches (white arrowheads) between the HM and VNC. CaP axons reach VM by 30 hpf (H) and ectopic branches appear to be retracting. By 36 hpf (I), CaP axons are extending branches along the ventral myotome; ectopic branches still remain but seem less numerous. J-L. In *ntn2* SBMO injected embryos CaP axons extend to VNC by 24 hpf (J) but one CaP axon has an ectopic branch (white arrowhead) By 30 hpf CaP axons extend to the VM (K); CaP axons are extending around the ventral aspect of the ventral myotome by 36 hpf (L). Dashed line represents the level of the HM. Abbreviation: bp, basepair.



Ntn1a is necessary for VaP axons to stop at the horizontal myoseptum

Netrins can act as either positive or negative cues for axons (Chilton, 2006). Although Netrins appear unnecessary to attract CaP axons to intermediate targets, the possibility remained that Ntn1a from the muscle pioneers might act to prevent the VaP axon from extending farther ventrally. To test this possibility, we knocked down Ntn1a function with a splice-blocking MO (Suli et al., 2006) and observed individually labeled CaPs and VaPs. Since *ntn1a* is expressed in muscle pioneers and muscle pioneers are necessary for VaP development (Eisen and Melançon, 2001) we first checked whether muscle pioneers were present in *ntn1a* MO-injected embryos. Embryos with reduced *ntn1a* transcript levels have muscle pioneers (Fig. 3B; see also Suli, 2007). We then followed the development of five dye-labeled pairs of CaPs and VaPs in *ntn1a*-MO injected embryos between 24 and 36 hpf. At 24 hpf, four of the five labeled VaP axons had branches extending along, but not beyond the horizontal myoseptum (data not shown). At 36 hpf all five labeled VaP axons in *ntn1a* MO-injected embryos extended beyond the horizontal myoseptum (Fig. 3D). This is in contrast to VaPs in standard control (Fig. 3C) and *ntn1a* mispair control (data not shown) MO-injected embryos in which VaP axons remained stalled at the muscle pioneers. We refer to these cells with axons extending beyond muscle pioneers and whose axon length is intermediate between a CaP axon and a VaP axon as “CaP-like” (Fig. 3D, red cell). Surprisingly, our time-lapse observations showed that when Ntn1a is absent, the identity of cells as CaPs or VaPs appears dynamic. For example, in the pair of cells shown in Fig. 3D, at 25 hpf, the green cell’s axon was stalled near muscle pioneers and the red cell’s axon extended into ventral muscle (Fig. 3D’). However, by 31 hpf, the red cell’s axon had retracted to the horizontal myoseptum and the green cell’s axon had extended into ventral muscle (Fig. 3D’). This kind of dynamic change between CaP and VaP identity was not

previously seen in timelapse observations of many VaPs under normal conditions (Eisen, 1992; Eisen and Melançon, 2001; Eisen et al., 1990).

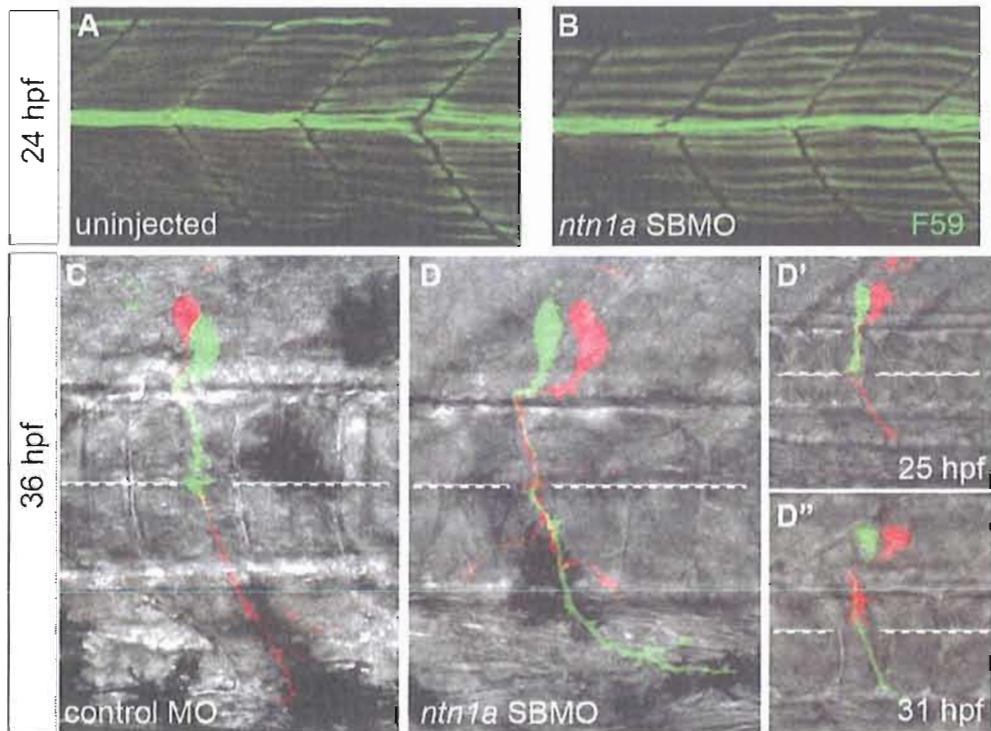


Fig. 3. *Ntn1a* is necessary for VaP axons to stop at the horizontal myoseptum. Confocal stacks of (A) uninjected and (B) *ntn1a* SBMO injected embryos labeled with F59, a slow muscle fiber marker. At 24 hpf, muscle pioneers (green fibers in the middle of the images) are present in both control and MO-injected embryos. C-D". Confocal stacks of living dye-labeled motoneurons. (C) VaP axons stalled at muscle pioneers at 36 hpf in standard control MO injected embryos. (D) *ntn1a* SBMO injected embryos showing CaP-like axon (red) extended beyond the muscle pioneers. D'-D". The same CaP and VaP pair shown in D. (D') At 25 hpf the red cell has developed as CaP. (D'') By 31 hpf the red cell had retracted its axon to the HM and the green cell now developed as CaP. Dashed line represents the level of the HM.

The CaP-like cell axons in *ntn1a* MO-injected embryos never extended as far as normal CaP axons and typically stopped at the ventral aspect of the notochord, suggesting additional genes may function to prevent the VaP axon from extending farther ventrally. Since ventral myotome at the level of the hypochord is an intermediate target for CaP axons (Beattie et al., 2000) we hypothesized that Netrins expressed in intermediate target regions

ventral to the horizontal myoseptum may function to restrict entry of axons of CaP-like cells into ventral muscle.

Netrins act together to restrict CaP-like axon entry into ventral muscle

To determine whether additional Netrins may function to restrict CaP-like axon extension into ventral muscle, we knocked down Ntn1b and Ntn2 individually and in combination with Ntn1a. We used a splice-blocking MO to knock down Ntn1b and followed three dye-labeled CaP and VaP pairs for 12 hours. Labeled VaPs did not extend beyond muscle pioneers (Fig. 4A). We knocked down Ntn2 with a splice-blocking MO (*ntn2* MO3; Suli, 2007) and followed four dye-labeled CaP and VaP pairs for 12 hours to learn whether reduction of Ntn2 leads to axon defects. Axons of all four VaPs were stalled at muscle pioneers at 36 hpf (Fig. 4B). Together these results provide evidence that neither Ntn1b nor Ntn2 alone is necessary for the VaP axon to stop at the horizontal myoseptum.

Having shown that neither Ntn1b nor Ntn2 was necessary for VaP axons to stop at the horizontal myoseptum, we then asked whether either of these Netrins might function to prevent a second CaP axon from extending toward more distal intermediate targets, forcing the cell to become CaP-like. To test this hypothesis, we followed three dye-labeled pairs of CaPs and VaPs in *ntn1a* plus *ntn1b* MO-injected embryos for 12 hours. At 24 hpf, one labeled VaP axon extended into ventral muscle, becoming CaP-like while the remaining VaP axons were stalled at the horizontal myoseptum (data not shown). However, by 36 hpf, all three VaP axons extended beyond the horizontal myoseptum, becoming CaP-like (Fig. 4C). Interestingly, the one CaP-like axon that extended farthest into ventral muscle retracted to a region near the hypochord. Since *ntn2* mRNA is present in ventral muscle, Ntn2 may have prevented the longest CaP-like axon from remaining in the ventral muscle, and may also

have prevented the other CaP-like axons from extending beyond the region of the hypochord, the vicinity of the second CaP intermediate target (Beattie et al., 2000). To test whether Ntn1a and Ntn2 function together to prevent the VaP axon from extending into ventral muscle, we injected embryos with *ntn1a* plus *ntn2* splice blocking MOs. We followed five dye-labeled pairs of CaPs and VaPs to 36 hpf. All five labeled VaP axons extended beyond the horizontal myoseptum, and two of those axons extended into ventral muscle (Fig. 4D); in these two cases both cells resembled normal CaPs. Taken together, these results suggest that Netrins function in combination to prevent a second CaP axon from extending into ventral muscle. The second CaP axon is normally stopped at the first intermediate target by Ntn1a, forcing the cell to become VaP. However, in the absence of Ntn1a, Ntn1b and/or Ntn2 function to prevent extension of the second CaP axon farther into CaP muscle territory.

The Dcc Netrin receptor is necessary for VaP axons to stop at the horizontal myoseptum

Depending on which Netrin receptors a cell expresses, Netrins can affect neurons differently. To determine whether differences in receptor distribution on CaP and VaP might contribute to their differential response to Netrins, we analyzed expression of several Netrin receptor genes, *dcc* (Fricke and Chien, 2005), *neo1* (Mawdsley et al., 2004), *neo2*, and *unc5b* (Lu et al., 2004). Of these genes, we found that only *dcc* is expressed in motoneurons; it is expressed in both CaP and VaP at 18 hpf and later (Fig. 5A).

We knocked down Dcc with a translation blocking MO (Suli et al., 2006) to test whether it is required for VaP axons to stop at the horizontal myoseptum. CaP axon extension was not altered by loss of Dcc (red cells in Fig. 5B-D). Muscle pioneers also appeared normal in the absence of Dcc (data not shown; Suli, 2007). We followed five dye-

labeled pairs of CaPs and VaPs in *dcc* MO-injected embryos between 24 and 36 hpf. At 24 hpf, none of the labeled VaP axons had extended beyond muscle pioneers (Fig. 5B). At 30 hpf, three of the five labeled VaP axons extended beyond the horizontal myoseptum (data not shown), but two of five remained in the region (Fig. 5C). By 36 hpf, four of the five labeled VaP axons extended beyond the horizontal myoseptum (Fig. 5D); thus, in the absence of Dcc VaPs became CaP-like. These results suggest that Dcc participates in mediating the ability of VaP to respond to Netrins. However, because none of the VaPs became CaPs, these results also suggest that additional Netrin receptors are likely to be involved.

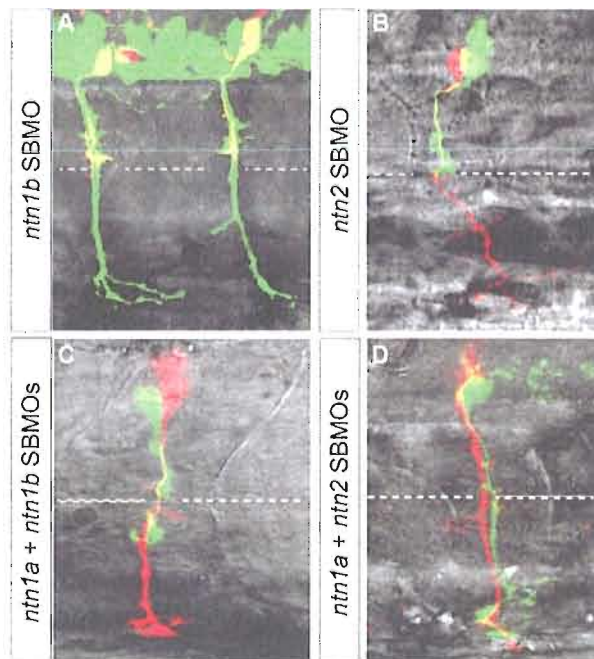


Fig. 4. Netrins act together to restrict extension of a second CaP axon into ventral muscle. Confocal stacks of living dye-labeled motoneurons in embryos injected with various combinations of MOs. A. *ntn1b* SBMO injected *Tg(mnx1:GFP)* embryo showing motoneurons (green) and rhodamine-dextran labeled VaPs (yellow). At 36 hpf the VaP axons are still stopped at muscle pioneers. B-D. Embryos with individually labeled pairs of CaP and VaP. In each case the CaP is red B. VaP axon (green) stopped at the muscle pioneers in *ntn2* SBMO injected embryo. C. A CaP-like axon (green) extends beyond the muscle pioneers to approximately the level of the hypochord in *ntn1a* plus *ntn1b* MO injected embryo. D. A second CaP axon (green) extends into ventral muscle in the absence of *ntn1a* and *ntn2*. Dashed line represents level of the HM.

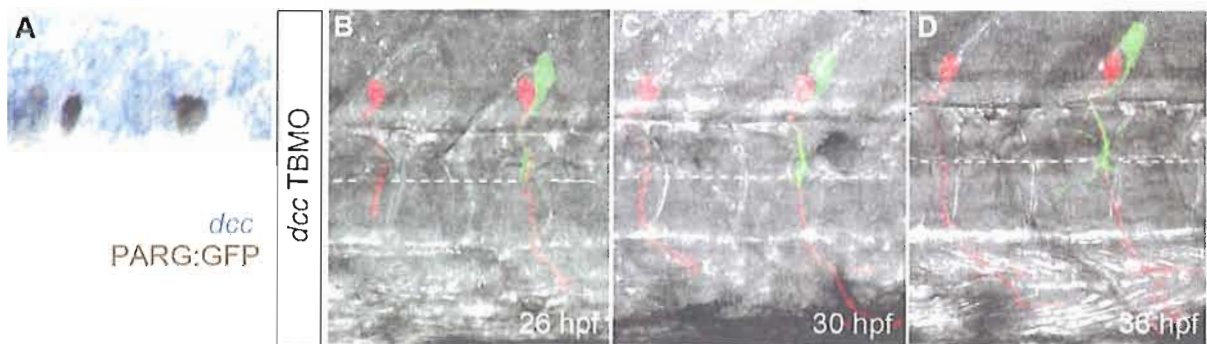


Fig. 5. Dcc is necessary for VaP axons to stop at muscle pioneers. A. Brightfield image of lateral view of zebrafish trunk focusing on the spinal cord. At 24 hpf *dcc* mRNA (blue) is co-localized with a motoneuron marker (PARG:GFP, brown). The anterior segment shows only CaP expressing *dcc* in a segment lacking VaP. The posterior segment shows that both CaP and VaP express *dcc*. B-D. Confocal stacks of living dye-labeled motoneurons in the same *dcc* TBMO injected embryo at several developmental stages. The anterior segment shows a CaP in a segment lacking VaP; the posterior segment shows both CaP and VaP. B. At 26 hpf the VaP axon (green) does not extend beyond the muscle pioneers but CaP axons (red) do extend farther. C. By 30 hpf, CaP axons have reached the VM but the VaP axon still remains near muscle pioneers. D. By 36 hpf, CaP axons have reached the ventral aspect of the ventral myotome, providing evidence that Dcc is unnecessary for CaP axon extension. The VaP axon now extends branches beyond muscle pioneers, but not beyond the level of the hypochord, becoming CaP-like. Dashed line represents level of the HM.

Existing anti-NETRIN and anti-DCC antibodies are not cross-reactive for zebrafish proteins

We and others (C.-B. Chien, personal communication) screened several commercially available anti-NETRIN and anti-DCC antibodies generated against mouse sequences, but none were cross reactive in whole mount zebrafish immunohistochemistry. Thus, we decided to generate rabbit polyclonal peptide antibodies unique to individual zebrafish Netrins. The resulting Ntn1a, Ntn1b and Ntn2 antisera were specific by ELISA assay to the appropriate sequences (data not shown). However, when Ntn1a and Ntn2 antisera were used in whole mount immunohistochemistry they did not produce specific staining (data not shown). Ntn1b antisera did yield staining in whole mount immunohistochemistry (data not shown) but the staining pattern is unexpected given *ntn1b* mRNA distribution, indicating that we did not produce anti-Netrin antibodies. We have

begun to collaborate with NeuroMAB to produce mouse monoclonal antibodies against full length zebrafish Netrin and Dcc proteins. After these antibodies are validated, they will be made generally available to the neuroscience community in accordance with NeuroMAB's policy to provide low cost, high quality mouse monoclonal antibodies to the neuroscience community (<http://www.neuromab.org/>).

Discussion

Netrins do not function as long-range cues to attract CaP axons to intermediate targets

Netrins act as guidance cues for specific motor axons in both vertebrates (Burgess et al., 2006; Varela-Echavarria et al., 1997) and invertebrates (Mitchell et al., 1996). Because of the expression patterns of zebrafish *netrin* mRNAs, we hypothesized that zebrafish Netrins function during CaP axon outgrowth to attract the CaP axon to its intermediate targets en route to ventral muscle. Generating anti-Netrin antibodies will enable us to analyze protein rather than mRNA distribution and thus provide further insight into how Netrins proteins function in vivo. Direct evidence for Netrin-1 function as a long distance guidance cue for commissural neurons comes from analysis of Netrin-1 protein distribution in embryonic chick spinal cords using pan-Netrin and Netrin-specific antibodies (Kennedy et al., 2006). Netrins function within the spinal cord to guide dorsally located commissural interneuron axons ventrally to floorplate and then across the midline to contralateral targets (Kennedy et al., 2006; Serafini et al., 1996). Netrin-1 mRNA is restricted to the floorplate, but immunohistochemistry revealed that Netrin-1 protein distribution extends several cell diameters dorsally of the floorplate, suggesting that a Netrin-1 gradient guides commissural axons ventrally (Kennedy et al., 2006). Analysis of protein distribution in chicks also revealed that, unlike Netrin-1, Netrin-2 may function as a gradient; Netrin-2 distribution is

similar to Netrin-2 mRNA distribution (Kennedy et al., 2006). The mouse genome lacks *Netrin-2*, but Netrin-1 protein expression is the sum of chick Netrin-1 and Netrin-2 protein expression (Kennedy et al., 2006, Serafini et al., 1996) suggesting Netrins function similarly among vertebrates.

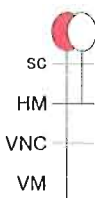


Zebrafish *ntn1a*, *ntn1b*, and *ntn2* are expressed in intermediate targets along the path of CaP axon outgrowth, and thus are poised to serve as attractive cues for the CaP axon as it extends ventrally. However, we found that in the absence of Netrins, the CaP axon successfully reached its intermediate targets, suggesting that Netrins do not attract CaP axons ventrally from afar. Instead, Netrins may function locally, at intermediate targets, as in the mouse retina (Deiner et al., 1997). Deiner et al. (1997) observed that in *Netrin* mutants, retinal ganglion cell axons projected correctly to intermediate targets, but once there extended aberrant axons that invaded neighboring tissue. Some CaP axons in embryos lacking *Ntn1b* or *Ntn2* also extended ectopic branches. Thus, Netrins may not function at a distance to guide axons but act locally to prevent exuberant branching.

Netrins restrict VaP axon extension into ventral muscle

While Netrins may not function as attractive guidance cues for CaP axons, our results suggest that they function to prevent a second CaP axon from entering ventral myotome (Table 2). *Ntn1a* is required for a second CaP axon to stop at the muscle pioneers, turning the cell into a VaP. Surprisingly, as revealed by double knock down experiments, *Ntn2* but not *Ntn1b* functions to prevent a second CaP axon from passing beyond the VNC intermediate target, causing the cell to become what we have termed CaP-like, a cell with an axon essentially intermediate between a CaP axon and a VaP axon. CaP-like axons in *ntn1a* plus *ntn1b*-MO-injected embryos do not extend as far ventrally as CaP-like axons in *ntn1a*

plus *ntn2*-MO-injected embryos. This result suggests that Ntn1b is unnecessary to prevent extension of VaP axons. Alternatively, Ntn1b and Ntn2 may function redundantly to prevent axons from extending beyond the VNC intermediate target. Transcripts of *ntn1b* and *ntn2* are expressed at the same axial level. However, *ntn1b* mRNA is expressed medially, in hypochord cells adjacent to the VNC, whereas *ntn2* mRNA is expressed laterally, in muscle cells adjacent to the VNC. Antibodies to the Ntn1b and Ntn2 proteins will be important reagents for resolving whether these proteins act locally or at a distance.

Table 2. Netrin signaling is necessary to prevent a second CaP axon from extending into ventral muscle. We observed three categories of axon phenotypes in MO injected embryos: Category I, CaP axons extend into ventral muscle and VaP axons extend no further than muscle pioneers. The majority of labeled CaP and VaPs pairs in standard control, *ntn1a* 5-mispair, *ntn1b*, and *ntn2* MO injected embryos were Category I (14/16). Category II, CaP axons extend into ventral muscle and a second CaP-like axon extends beyond the muscle pioneers, but no further than the hypochord. Almost all the labeled CaP and VaP pairs in *ntn1a* and *dcc* MO injected embryos were Category II (9/10). Knocking down Ntn1a and Ntn1b in combination yielded only Category II cases (3/3). Category III, both CaP and VaP extend axons into ventral muscle, thus both cells develop as CaPs. Knocking down Ntn2 in combination with Ntn1a resulted in several Category III cells (2/5). *ntn1a* plus *ntn2* MO injected embryos were not followed beyond 36 hpf, thus axon outgrowth in the 3 Category II cases could have been delayed as a consequence of multiple MOs.

MO injected	Category I 	Category II 	Category III 	Total
standard control MO	5	1	0	6
<i>ntn1a</i> 5-mispair MO	3	0	0	3
<i>ntn1a</i> SBMO	0	5	0	5
<i>ntn1b</i> SBMO	2	1	0	3
<i>ntn1a</i> plus <i>ntn1b</i> SBMOs	0	3	0	3
<i>ntn2</i> SBMO	4	0	0	4
<i>ntn1a</i> plus <i>ntn2</i> SBMOs	0	3	2	5
<i>dcc</i> TBMO	1	4	0	5

Refining a two signal model for VaP development

Previous work describing interactions between CaP, muscle pioneers, and VaP indicated that at least two signals are required for VaP development, a CaP-derived signal, which may act between CaP and muscle pioneers, and a muscle pioneer-derived signal, which may act between muscle pioneers and VaP to prevent a second CaP axon from extending ventrally (Eisen and Melançon, 2001). Alternatively, the CaP-derived signal may act between CaP and VaP, while the muscle pioneer-derived signal may act between muscle pioneers and VaP. Resolving the molecular identity of the CaP-derived and muscle pioneer-derived signals and subsequent genetic analysis will enable us to determine when and where each signal acts to contribute to VaP formation. Although we have not yet resolved the timing of the CaP-derived and muscle pioneer-derived signals, we have identified a muscle pioneer-derived molecular signal necessary to stop VaP axons from extending beyond muscle pioneers. To search for this signal we considered molecules that act as bifunctional cues that can both attract and repel axons. We envisioned that such a cue could allow the first CaP axon to extend beyond muscle pioneers, but then prevents a second CaP from following the same route, thus forcing the cell to become a VaP.

Ntn1a is a muscle pioneer-derived signal necessary for VaP axons to stop at muscle pioneers

Netrin can switch between functioning as a repulsive cue and functioning as an attractive cue for the same axon, depending on levels of cyclic AMP (cAMP) (Shewan et al., 2002), the ratio of cAMP to cGMP (Nishiyama et al., 2003), or the specific Netrin receptors on the cell surface (Chilton, 2006). Dcc mediates axon attraction whereas co-expression of Dcc and another Netrin receptor, Unc5b, mediates repulsion (Hong et al., 1999). The choice between CaP and VaP fates requires that the VaP axon stall at the muscle pioneers. It is

likely that Netrin signaling only works locally at intermediate targets to permit CaP axon and to restrict VaP axon passage, but that another set of guidance molecules provide cues for axon extension. A simple model for CaP and VaP formation is that since both CaP and VaP express *dcc* mRNA, Netrin is attractive for CaP and VaP axons locally at the muscle pioneers. However, we have shown that Netrin is unnecessary for the CaP and VaP axons to extend to the muscle pioneers, suggesting that any attraction is mediated by other signals. Interactions between CaP, VaP and muscle pioneers could act to alter Netrin receptor distribution in such a way that the VaP axon remains stalled at the muscle pioneers. This could result from the VaP axon becoming attracted to Netrin, and thus remaining at the source. Alternatively, it could result from the VaP axon becoming repelled by Netrin, and thus being unable to progress beyond a Netrin source. Distinguishing between these alternatives will require detailed knowledge of Netrin and Dcc protein distributions. However, previous work from the lab showed that VaP growth cones become enlarged as they contact the muscle pioneers (Dent et al., 2004). These observations are not consistent with the growth cone collapse typically associated with growth cone repulsion (Dent et al., 2004). Thus, our working model is that VaP growth cones stall at the muscle pioneers because they become attracted to these *Ntn1a*-secreting cells. One possibility that we hope to explore in the future with antibodies is that contact between CaP and the muscle pioneers is required for secretion of *Ntn1a*.

Recent work in rat neuronal cultures demonstrated that inhibition of RhoA GTPase signaling increases plasma membrane bound Dcc and increases Netrin responsiveness (Moore et al., 2008). While *ntn1a* mRNA is expressed in muscle pioneers and *dcc* mRNA is expressed in both motoneurons before CaP and VaP axon outgrowth, Netrin signaling appears dispensable for VaP development until CaP and VaP axons arrive at muscle

pioneers. CaP may not respond to Netrin because its axon does not have any Dcc protein localized to the plasma membrane. However, passage of the CaP axon past the muscle pioneers might cause Dcc to be localized to the VaP axon plasma membrane. Consequently, the VaP axon, but not the CaP axon is able to respond to Netrin signaling from muscle pioneers. Manipulating RhoA GTPase levels in CaP and VaP may also provide insight into signals that distinguish the two cells.

Significance of Netrin signaling for motoneuron development

It is clear that Ntn1a functions to prevent VaP axons from extending beyond muscle pioneers. However, since *ntn1b* and *ntn2* mRNAs are expressed ventrally to the muscle pioneers they cannot function to restrict an errant VaP axon from extending into this region unless they are secreted over a long distance, as our future antibody studies will reveal. So do these Netrins have a normal role in motor axon outgrowth? RoP, another zebrafish primary motoneuron, and subpopulations of later-developing secondary motoneurons innervate axial muscle that overlays the region between the level of the horizontal myoseptum and the ventral aspect of the notochord (Eisen et al., 1986; Myers et al., 1986; Westerfield et al., 1986). Thus, it seems likely that, rather than acting to restrict VaP axon outgrowth, Ntn1b and Ntn2 normally function to restrict axon outgrowth of RoP and at least some secondary motoneurons to ensure region-specific muscle innervation.

Conclusion

Our results provide evidence that Netrins do not function at a distance to guide zebrafish motoneuron axons. Rather, Netrin signaling is required locally at the first intermediate target of the CaP axon pathway to prevent a second CaP axon from extending

beyond this region, forcing the cell to become VaP and follow a different course of development. Other Netrins are likely to restrict additional motoneuron axons from projecting ventrally, ensuring the development of cell-appropriate arbors that innervate correct targets.

CHAPTER V

CONCLUSION

Retinoic acid signaling in patterning and specifying the zebrafish nervous system

My survey of retinoic acid and retinoid X receptor mRNA distribution revealed that patterning and specification of motoneurons in the zebrafish spinal cord by retinoic acid is not the consequence of unique receptor distribution. In general, within the spinal cord, mRNA for retinoic acid and retinoid X receptors was not specific for any one motoneuron subpopulation. Instead, retinoic acid signaling in specific cell types may be achieved by the presence of molecules that are either involved in retinoic acid synthesis or degradation.

Making the right neuronal connections with Netrins

My analysis of Netrin signaling in motoneuron development led to the discovery that Netrins function to refine the CaP-specific axon arbor. They may also function to refine axon territories of RoPs and later-developing secondary motoneurons. In the absence of Netrins, at least two CaP motoneurons can project to the same target. It would be interesting to determine whether both cells maintain their ventral muscle innervation, if one cell later dies because the ventral muscle is unable to support two cells in the region due to lack of trophic support (see discussion in Eisen and Melançon, 2001), or if the two cells divide up the innervation territory, as has been described for tiling of sensory neurons in *Drosophila melanogaster* (Soba et al., 2007; Grueber et al., 2002). Preliminary data suggest that ventral muscle can support two cells in the region, but I have not extended my observations

to adults to determine whether two CaPs would persist. Another exciting future project would be to test whether Netrins are involved in determining innervation patterns of RoP and/or secondary motoneurons. Virtually nothing is known about how these cells select their arborization territories, and with the exception of early electrophysiological studies from adults, almost nothing is known about the innervation patterns of subsets of secondary motoneurons. Finally, it would be interesting to determine the consequence to motor behavior of having multiple motoneurons innervating the same region. Discovering that behavior is unaffected would have important consequences for understanding plasticity within developing nervous systems.

REFERENCES

Chapter I

- Appel, B. and Eisen, J.S., 2003. Retinoids Run Rampant: Multiple Roles during Spinal Cord and Motor Neuron Development. *Neuron* 40, 461-64.
- Begemann, G., Marx, M., Mebus, K., Meyer, A and Bastmeyer, M., 2004. Beyond the neckless phenotype: influence of reduced retinoic acid signaling on motor neuron development in the zebrafish hindbrain. *Dev. Biol.* 271, 119-29.
- Concordet, J.P. and Ingham, P. (1995). Developmental biology. Patterning goes sonic. *Nature* 375, 279-80.
- Eisen, J.S. and Melançon, E. (2001). Interactions with identified muscle cells break motoneuron equivalence in embryonic zebrafish. *Nat. Neurosci.* 4, 1065-70.
- Goncalves, M.B., Boyle, J., Webber, D., Hall, S., Minger, S.L. and Corcoran, P.T., 2005. Timing of retinoid-signaling pathway determines the expression of neuronal markers in neural progenitor cells. *Dev. Biol.* 278, 60-70.
- Grueber, W.B., Jan, L.Y. and Jan, Y.N. (2002). Tiling of the *Drosophila* epidermis by multidendritic sensory neurons. *Development* 129, 2867-78.
- Linville, A., Gumusaneli, E., Chandraratna, R.A.S. and Schilling, T.F., 2004. Independent roles for retinoic acid in segmentation and neuronal differentiation in the zebrafish hindbrain. *Dev. Biol.* 270, 186-99.
- Maden, M., 2002. Retinoid Signalling in the Development of the Central Nervous System. *Nat. Rev. Neurosci.* 3, 843-53.
- Soba, P., Zhu, S., Emoto, K., Younger, S., Yang, S.J., Yu, H.H., Lee, T., Jan, L.Y. and Jan, Y.N. (2007). *Drosophila* sensory neurons require Dscam for dendritic self-avoidance and proper dendritic field organization. *Neuron* 54, 403-16.
- Sokanathan, S., Perlmann, T. and Jessell, T.M., 2003. Retinoid receptor signaling in postmitotic motor neurons regulates rostrocaudal positional identity and axonal projection pattern. *Neuron* 40, 97-111.

Chapter II

- Akimenko, M.-A., Ekker, M., Wegner, J., Lin, W. and Westerfield, M., 1994. Combinatorial expression of three zebrafish genes related to Distalless: part of a homeobox gene code for the head. *J. Neurosci.* 14, 3475-3486.
- Amores, A., Force, A., Yan, Y.-L., Joly, L., Amemiya, C., Fritz, A., Ho, R.K., Langeland, J., Prince, V., Wang, Y.-L., Westerfield, M., Ekker, M. and Postlethwait, J.H., 1998. Zebrafish hox clusters and vertebrate genome evolution. *Science* 282, 1711-4.
- Appel, B. and Eisen, J.S., 2003. Retinoids Run Rampant: Multiple Roles during Spinal Cord and Motor Neuron Development. *Neuron* 40, 461-64.
- Bastien, J. and Rochette-Egly, C., 2004. Nuclear retinoid receptors and the transcription of retinoid-target genes. *Gene* 328, 1-16.
- Begemann, G., Marx, M., Mebus, K., Meyer, A. and Bastmeyer, M., 2004. Beyond the neckless phenotype: influence of reduced retinoic acid signaling on motor neuron development in the zebrafish hindbrain. *Dev. Biol.* 271, 119-29.
- Begemann, G., Schilling, T.F., Rauch, G.-J., Geisler, R. and Ingham, P.W., 2001. The zebrafish neckless mutation reveals a requirement for raldh2 in mesodermal signals that pattern the hindbrain. *Development* 128, 3081-94.
- Gavalas, A. and Krumlauf, R., 2000. Retinoid signalling and hindbrain patterning. *Curr. Opin. Genet. Dev.* 10, 380-6.
- Goncalves, M.B., Boyle, J., Webber, D., Hall, S., Minger, S.L. and Corcoran, P.T., 2005. Timing of retinoid-signaling pathway determines the expression of neuronal markers in neural progenitor cells. *Dev. Biol.* 278, 60-70.
- Grandel, H., Lun, K., Rauch, G.J., Rhinn, M., Piotrowski, T., Houart, C., Sordino, P., Kuchler, A.M., Schulte-Merker, S., Geisler, R., Holder, N., Wilson, S.W. and Brand, M., 2002. Retinoic acid signalling in the zebrafish embryo is necessary during pre-segmentation stages to pattern the anterior-posterior axis of the CNS and to induce a pectoral fin bud. *Development* 129, 2851-65.
- Ghyselinck, N.B., Dupé, V., Dierich, A., Messaddeq, N., Garnier, J.M., Rochette-Egly, C., Chambon, P. and Mark, M., 1997. Role of the retinoic acid receptor beta (RARbeta) during mouse development.. *Int. J. Dev. Biol.* 41, 425- 47.

- Goodman, A.B., 2005. Microarray results suggest altered transport and lowered synthesis of retinoic acid in schizophrenia. *Mol. Psychiatry* 10, 620-1.
- Hauptmann, G. and Gerster, T., 1994. Two-colour whole-mount in situ hybridization to vertebrate and *Drosophila* embryos. *Trends Genet.* 10, 266.
- Jiang, X., Choudhary, B., Merki, E., Chien, K.R., Maxson, R.E. and Sucov, H.M., 2002. Normal fate and altered function of the cardiac neural crest cell lineage in retinoic acid receptor mutant embryos. *Mech. Dev.* 117, 115-22.
- Joore, J., van der Lans, G.B.L.J., Lanser, P.H., Vervaart, J.M.A., Zivkovic, D., Speksnijder and J.E., Kruijer, W., 1994. Effects of retinoic acid on the expression of retinoic acid receptors during zebrafish embryogenesis. *Mech. Dev.* 46, 137-50.
- Kimmel, C.B., Ballard, W.W., Kimmel, S.R., Ullmann, B. and Schilling, T.F., 1995. Stages of embryonic development of Zebrafish. *Dev. Dyn.* 203, 253-310.
- Krezel, W., Ghyselinck, N., Samad, T.A., Dupe, V., Kastner, P., Borrelli, E. and Chambon, P., 1998. Impaired locomotion and dopamine signaling in retinoid receptor mutant mice. *Science* 279, 863-7.
- Krust, A., Kastner, P.H., Petkovich, M., Zelent, A. and Chambon, P., 1989. A third human retinoic acid receptor, hRAR-gamma. *Proc. Natl. Acad. Sci.* 86, 5310-4.
- Lane, M.A. and Bailey, S.J., 2005. Role of retinoid signalling in the adult brain. *Prog. Neurobiol.* 75, 275-93.
- Linville, A, Gumusaneli, E., Chandraratna, R.A.S. and Schilling, T.F., 2004. Independent roles for retinoic acid in segmentation and neuronal differentiation in the zebrafish hindbrain. *Dev. Biol.* 270, 186-99.
- Maden, M., 2002. Retinoid Signalling in the Development of the Central Nervous System. *Nat. Rev. Neurosci.* 3, 843-53.
- Maden, M., Sonneveld, E., van der Saag, P.T. and Gale, E., 1998. The distribution of endogenous retinoic acid in the chick embryo: implications for developmental mechanisms. *Development* 125, 4133-44.
- Mangelsdorf, D.J., Thummel, C., Beato, M., Herrlich, P., Schutz, G., Umesono, K., Blumberg, B., Kastner, P., Mark, M., Chambon, P. and Evans, R.M., 1995. The nuclear receptor superfamily: the second decade. *Cell* 83, 835-9.

- Niederreither, K., Subbarayan, V., Dolle, P. and Chambon, P., 1999. Embryonic retinoic acid synthesis is essential for early mouse post-implantation development. *Nat. Genet.* 21, 444-8.
- Oxtoby, E. and Jowett, T., 1993. Cloning of the zebrafish *krox-20* gene (*krx-20*) and its expression during hindbrain development. *Nucleic Acid Res.* 21, 1087-95.
- Postlethwait, J.H., Yan, Y.-L., Gates, M., Horne, S., Amores, A., Brownlie, A., Donovan, A., Egan, E., Force, A., Gong, Z., Goutel, C., Fritz, A., Kelsh, R., Knapik, E., Liao, E., Paw, B., Ransom, D., Singer, A., Thomson, M., Abduljabbar, T.S., Yelick, P., Beier, D., Joly, J.-S., Larhammar, D., Rosa, F., Westerfield, M., Zon, L.I., Johnson, S.L. and Talbot, W.S., 1998. Vertebrate genome evolution and the zebrafish gene map. *Nat. Genet.* 18, 345-9.
- Rioux, L. and Arnold, S.E., 2005. The expression of retinoic acid receptor alpha is increased in the granule cells of the dentate gyrus in schizophrenia. *Psychiatry Res.* 133, 13-21.
- Ruberte, E., Dolle, P., Krust, A., Zelent, A., Morriss-Kay, G. and Chambon, P., (1990). Specific spatial and temporal distribution of retinoic acid receptor gamma transcripts during mouse embryogenesis. *Development* 108, 213-22.
- Ruberte, E., Friederich, V., Chambon, P. and Morriss-Kay, G., 1993. Retinoic acid receptors and cellular retinoid binding proteins III. Their differential transcript distribution during mouse nervous system development. *Development* 118, 267-82.
- Saitou, N. and Nei, M., 1987. The neighbor-joining method: a new method for reconstructing phylogenetic trees. *Mol. Biol. Evol.* 4, 406-25.
- Sharma, M.K., Saxena, V., Liu, R.-Z., Thisse, C., Thisse, B., Denovan-Wright, E.M. and Wright, J.M., 2005. Differential expression of the duplicated cellular retinoic acid-binding protein 2 genes (*crabp2a* and *crabp2b*) during zebrafish embryonic development. *Gene Expr. Patterns* 5, 371-9.
- Sokanathan, S., Perlmann, T. and Jessell, T.M., 2003. Retinoid receptor signaling in postmitotic motor neurons regulates rostrocaudal positional identity and axonal projection pattern. *Neuron* 40, 97-111.
- Soprano, K.J. and Soprano, D.R., 2002. Retinoic acid receptors and cancer. *J. Nutr.* 132, 3809S-13S.

- Sprague, J., Doerry, E., Douglas, S. and Westerfield, M., 2001. The Zebrafish Information Network (ZFIN): a resource for genetic, genomic and developmental research. *Nucleic Acids Res.* 29, 87-90.
- Taylor, J., Braasch, I., Frickey, T., Meyer, A. and Van De Peer, Y., 2003. Genome duplication, a trait shared by 22,000 species of ray-finned fish. *Genome Res.* 13, 382-90.
- Westerfield, M., 1995. *The zebrafish book: a guide for the laboratory use of zebrafish (Danio rerio)*. University of Oregon Press, Eugene, OR.
- White, J.A., Boffa, M.B., Jones, B.B. and Petkovich, M., 1994. A zebrafish retinoic acid receptor expressed in the regenerating caudal fin. *Development* 120, 1861-72.
- Woods, I.G., Kelly, P.D., Chu, F., Ngo-Hazelett, P., Yan, Y.L., Huang, H., Postlethwait, J.H. and Talbot, W.S., 2000. A comparative map of the zebrafish genome. *Genome Res.* 10, 1903-14.
- Zhao, Q., Dobbs-McAuliffe, B. and Linney, E., 2005. Expression of *cyp26b1* during zebrafish early development. *Gene Expr. Patterns* 5, 363-9.

Chapter III

- Amores, A., Force, A., Yan, Y.-L., Joly, L., Amemiya, C., Fritz, A., Ho, R.K., Langeland, J., Prince, V., Wang, Y.-L., Westerfield, M., Ekker, M. and Postlethwait, J.H., 1998. Zebrafish *hox* clusters and vertebrate genome evolution. *Science* 282, 1711-4.
- Bastien, J. and Rochette-Egly, C., 2004. Nuclear retinoid receptors and the transcription of retinoid-target genes. *Gene* 328, 1-16.
- Crowe, D.L. and Chandraratna, R.A.S., 2004. A retinoid X receptor (RXR)-selective retinoid reveals that RXR- α is potentially a therapeutic target in breast cancer cell lines, and that it potentiates antiproliferative and apoptotic responses to peroxisome proliferator-activated receptor ligands. *Breast Cancer Res.* 6, R546-R55.
- Dolle, P., Fraulob, V., Kastner, P. and Chambon, P., 1994. Developmental expression of murine retinoid X receptor (RXR) genes. *Mech. Dev.* 45, 91-104.
- Gavalas, A. and Krumlauf, R., 2000. Retinoid signalling and hindbrain patterning. *Curr. Opin. Genet. Dev.* 10, 380-6.

- Georgiades, P. and Brickell, P.M., 1997. Differential expression of the rat retinoid X receptor gamma gene during skeletal muscle differentiation suggests a role in myogenesis. *Dev. Dyn.* 210, 227-35.
- Ghose, R., Zimmerman, T.L., Thevananther, S. and Karpen, S.J., 2004. Endotoxin leads to rapid subcellular re-localization of hepatic RXRalpha: A novel mechanism for reduced hepatic gene expression in inflammation. *Nucl. Recept.* 2, 4.
- Grandel, H., Lun, K., Rauch, G.J., Rhinn, M., Piotrowski, T., Houart, C., Sordino, P., Kuchler, A.M., Schulte-Merker, S., Geisler, R., Holder, N., Wilson, S.W. and Brand, M., 2002. Retinoic acid signalling in the zebrafish embryo is necessary during pre-segmentation stages to pattern the anterior-posterior axis of the CNS and to induce a pectoral fin bud. *Development* 129, 2851-65.
- Hauptmann, G. and Gerster, T., 1994. Two-colour whole-mount in situ hybridization to vertebrate and Drosophila embryos. *Trends Genet.* 10, 266.
- Hoover, F., Seleiro, E.A., Kielland, A., Brickell, P.M. and Glover, J.C., 1998. Retinoid X receptor gamma gene transcripts are expressed by a subset of early generated retinal cells and eventually restricted to photoreceptors. *J. Comp. Neurol.* 391, 204-13.
- Hoover, F., Kielland, A. and Glover, J.C., 2000. RXR gamma gene is expressed by discrete cell columns within the alar plate of the brainstem of the chicken embryo. *J. Comp. Neurol.* 416, 417-28.
- Holland, P.W.H., Garcia-Fernàndez, J., Williams, N.A. and Sidow, A., 1994. Gene duplications and the origins of vertebrate development. *Development Suppl.*, 125-33.
- Jiang, X., Choudhary, B., Merki, E., Chien, K.R., Maxson, R.E. and Sucov, H.M., 2002. Normal fate and altered function of the cardiac neural crest cell lineage in retinoic acid receptor mutant embryos. *Mech. Dev.* 117, 115-22.
- Jones, B.B., Ohno, C.K., Allenby, G., Boffa, M.B., Levin, A.A., Grippo, J.P. and Petkovich, M., 1995. New Retinoid X Receptor Subtypes in Zebra Fish (*Danio rerio*) Differentially Modulate Transcription and Do Not Bind 9-cis Retinoic Acid. *Mol. Cell. Biol.* 15, 5226-34.
- Kastner, P., Mark, M., Ghyselinck, N., Krezel, W., Dupe, V., Grondona, J.M. and Chambon, P., 1997. Genetic evidence that the retinoid signal is transduced by heterodimeric RXR/RAR functional units during mouse development. *Development* 124, 313-26.

- Kawakami, Y., Raya, A., Raya, R.M., Rodriguez-Esteban, C. and Belmonte, J.C., 2005. Retinoic acid signalling links left-right asymmetric patterning and bilaterally symmetric somitogenesis in the zebrafish embryo. *Nature* 435, 165-71.
- Kelley, M.W., Turner, J.K. and Reh, T.A., 1995. Ligands of steroid/thyroid receptors induce cone photoreceptors in vertebrate retina. *Development* 121, 3777-85.
- Kimmel, C.B., Ballard, W.W., Kimmel, S.R., Ullmann, B. and Schilling, T.F., 1995. Stages of embryonic development of Zebrafish. *Dev. Dyn.* 203, 253-310.
- Le Douarin, N.M. and Smith, J., 1988. Development of the peripheral nervous system from the neural crest. *A. Rev. Cell. Biol.* 4, 375-404.
- Lewis, K.E. and Eisen, J.S., 2004. Paraxial mesoderm specifies zebrafish primary motoneuron subtype identity. *Development* 131, 891-902.
- Li, Y., Dawson, M.I., Agadir, A., Lee, M.O. and Jong, L., 1998. Regulation of RAR beta expression by RAR- and RXRselective retinoids in human lung cancer cell lines: effect on growth inhibition and apoptosis induction. *Int. J. Cancer* 75, 88-95.
- Mangelsdorf, D.J., Ong, E.S., Dyck, J.A. and Evans, R.M., 1990. Nuclear receptor that identifies a novel retinoic acid response pathway. *Nature* 345, 224-9.
- Mangelsdorf, D. J., Borgmeyer, U., Heyman, R. A., Zhou, J. Y., Ong, E. S., Oro, A. E., Kakizuka, A. and Evans, R. M., 1992. Characterization of three RXR genes that mediate the action of 9-cis retinoic acid. *Genes Dev.* 6, 329-44.
- Naruse, K., Tanaka, M., Mita, K., Shima, A., Postlethwait, J. and Mitani, H., 2004. A medaka gene map: the trace of ancestral vertebrate proto-chromosomes revealed by comparative gene mapping. *Genome Res.* 14, 820-8.
- Okuno, M., Kojima, S., Matsushima-Nishiwake, R., Tsurumi, H., Muto, Y., Friedmann, S.L. and Moriwaki, H., 2004. Retinoids in cancer chemoprevention. *Curr. Cancer Drug Targets* 4, 285-98.
- Oxtoby, E. and Jowett, T., 1993. Cloning of the zebrafish krox-20 gene (*krx-20*) and its expression during hindbrain development. *Nucleic Acid Res.* 21, 1087-95.

- Postlethwait, J.H., Yan, Y.-L., Gates, M.A., Horne, S., Amores, A., Brownlie, A., Donovan, A., Egan, E.S., Force, A., Gong, Z., Goutel, C., Fritz, A., Kelsh, R., Knapik, E., Liao, E., Paw, B., Ransom, D., Singer, A., Thomson, M., Abduljabbar, T.S., Yelick, P., Beier, D., Joly, J.-S., Larhammar, D., Rosa, F., Westerfield, M., Zon, L.I., Johnson, S.L. and Talbot, W.S., 1998. Vertebrate genome evolution and the zebrafish gene map. *Nature Genet.* 18, 345-9.
- Rowe, A., Eager, N.S. and Brickell, P.M., 1991. A member of the RXR nuclear receptor family is expressed in neural-crest-derived cells of the developing chick peripheral nervous system. *Development* 111, 771-8.
- Saitou, N. and Nei, M., 1987. The neighbor-joining method: a new method for reconstructing phylogenetic trees. *Mol. Biol. Evol.* 4, 406-25.
- Soprano, D.R., Qin, P. and Soprano, K.J., 2004. Retinoic acid receptors and cancers. *Review. Annu. Rev. Nutr.* 24, 201-21.
- Sprague, J., Doerry, E., Douglas, S. and Westerfield, M., 2001. The Zebrafish Information Network (ZFIN): a resource for genetic, genomic and developmental research. *Nucleic Acids Res.* 29, 87-90.
- Stratford, T., Horton, C. and Maden M., 1996. Retinoic acid is required for the initiation of outgrowth in the chick limb bud. *Curr. Biol.* 6, 1124-33.
- Strausberg, R.L., Feingold, E.A., Grouse, L.H., Derge, J.G., Klausner, R.D., Collins, F.S., Wagner, L., Shenmen, C.M., Schuler, G.D., Altschul, S.F., Zeeberg, B., Buetow, K.H., Schaefer, C.F., Bhat, N.K., Hopkins, R.F., Jordan, H., Moore, T., Max, S.I., Wang, J., Hsieh, F., Diatchenko, L., Marusina, K., Farmer, A.A., Rubin, G.M., Hong, L., Stapleton, M., Soares, M.B., Bonaldo, M.F., Casavant, T.L., Scheetz, T.E., Brownstein, M.J., Usdin, T.B., Toshiyuki, S., Carninci, P., Prange, C., Raha, S.S., Loquellano, N.A., Peters, G.J., Abramson, R.D., Mullahy, S.J., Bosak, S.A., McEwan, P.J., McKernan, K.J., Malek, J.A., Gunaratne, P.H., Richards, S., Worley, K.C., Hale, S., Garcia, A.M., Gay, L.J., Hulyk, S.W., Villalon, D.K., Muzny, D.M., Sodergren, E.J., Lu, X., Gibbs, R.A., Fahey, J., Helton, E., Kettelman, M., Madan, A., Rodrigues, S., Sanchez, A., Whiting, M., Madan, A., Young, A.C., Shevchenko, Y., Bouffard, G.G., Blakesley, R.W., Touchman, J.W., Green, E.D., Dickson, M.C., Rodriguez, A.C., Grimwood, J., Schmutz, J., Myers, R.M., Butterfield, Y.S., Krzywinski, M.I., Skalska, U., Smailus, D.E., Schnerch, A., Schein, J.E., Jones, S.J. and Marra, M.A., 2002. Generation and initial analysis of more than 15,000 full-length human and mouse cDNA sequences. *Proc. Natl. Acad. Sci. U.S.A.* 99, 16899-903.

- Taylor, J.S., Braasch, I., Frickey, T., Meyer, A. and Van de Peer, Y., 2003. Genome duplication, a trait shared by 22000 species of ray-finned fish. *Genome Res.* 13, 382-90.
- Thisse, B. and Thisse, C., 2004. Fast Release Clones: A High Throughput Expression Analysis. ZFIN Direct Data Submission.
- Umesono K. and Evans R.M., 1989. Determinants of target gene specificity for steroid/thyroid hormone receptors. *Cell* 57, 1139-46.
- Westerfield, M., 1995. *The zebrafish book: a guide for the laboratory use of zebrafish (Danio rerio)*. University of Oregon Press, Eugene, OR
- White, J.A., Boffa, M.B., Jones, B.B. and Petkovich, M., 1994. A zebrafish retinoic acid receptor expressed in the regenerating caudal fin. *Development.* 120, 1861-72.
- Willy, P.J. and Mangelsdorf, D.J., 1999. Nuclear orphan receptors: the search for novel ligands and signaling pathways. In: O'Malley, B.W. (Ed.), *Hormone and Signaling*. Academic Press, San Diego, 307-58.
- Woods, I.G., Kelly, P.D., Chu, F., Ngo-Hazelett, P., Yan, Y.L., Huang, H., Postlethwait, J.H. and Talbot, W.S., 2000. A comparative map of the zebrafish genome. *Genome Res.* 10, 1903-14.
- Woods, I.G., Wilson, C., Friedlander, B., Chang, P., Daengnoy K., Reyes, D.G., Nix, R., Kelly, P.D., Chu, F., Postlethwait, J.P. and Talbot, W.S., 2005. The zebrafish gene map defines ancestral vertebrate chromosomes. *Genome Res.* 15, 1307-14.
- Zetterstrom, R.H., Lindqvist, E., Mata de Urquiza, A., Tomac, A., Eriksson, U., Perlmann, T. and Olson, L., 1999. Role of retinoids in the CNS: differential expression of retinoid binding proteins and receptors and evidence for presence of retinoic acid. *Eur. J. Neurosci.* 11, 407-16.
- Zhang, X., Odom, D.T., Koo, S.-H., Conkright, M.D., Canettieri, G., Best, J., Chen, H., Jenner, R., Herbolsheimer, E., Jacobsen, E., Kadam, S., Ecker, J.R., Emerson, B., Hogenesch, J.B., Unterman, T., Young, R.A. and Montminy, M., 2005. Genome-wide analysis of cAMP-response element binding protein occupancy, phosphorylation, and target gene activation in human tissues. *Proc. Natl. Acad. Sci.* 102, 4459-64.

Chapter IV

- Appel, B. and Eisen, J.S. (1998). Regulation of neuronal specification in the zebrafish spinal cord by Delta function. *Development* 125, 371-80.
- Appel, B., Givan, L.A. and Eisen, J.S. (2001). Delta-Notch signaling and lateral inhibition in zebrafish spinal cord development. *BMC Dev. Biol.* 1, 13.
- Balciunas, D., Davidson, A.E., Sivasubbu, S., Hermanson, S.B., Welle, Z. and Ekker, S.C. (2004). Enhancer trapping in zebrafish using the Sleeping Beauty transposon. *BMC Genomics* 5, 62.
- Beattie, C.E., Melançon, E. and Eisen, J.S. (2000). Mutations in the stumpy gene reveal intermediate targets for zebrafish motor axons. *Development* 127, 2653-62.
- Burgess, R.W., Jucius, T.J. and Ackerman, S.L. (2006). Motor axon guidance of the mammalian trochlear and phrenic nerves: dependence on the netrin receptor *Unc5c* and modifier loci. *J. Neurosci.* 26, 5756-66.
- Chilton, J.K. (2006). Molecular mechanisms of axon guidance. *Dev. Biol.* 292, 13-24.
- Crow, M.T. and Stockdale, F.E. (1986). Myosin expression and specialization among the earliest muscle fibers of the developing avian limb. *Dev. Biol.* 113, 238-54.
- Deiner, M.S., Kennedy, T.E., Fazeli, A., Serafini, T., Tessier-Lavigne, M. and Sretavan, D.W. (1997). Netrin-1 and DCC mediate axon guidance locally at the optic disc: loss of function leads to optic nerve hypoplasia. *Neuron* 19, 575-89.
- Dent, E.W., Barnes, A.M., Tang, F. and Kalil, K. (2004). Netrin-1 and semaphorin 3A promote or inhibit cortical axon branching, respectively, by reorganization of the cytoskeleton. *J. Neurosci.* 24, 3002-12.
- Devoto, S.H., Melançon, E., Eisen, J.S. and Westerfield, M. (1996). Identification of separate slow and fast muscle precursor cells in vivo, prior to somite formation. *Development* 122, 3371-80.
- Eisen, J.S. (1992). The role of interactions in determining cell fate of two identified motoneurons in the embryonic zebrafish. *Neuron* 8, 231-40.
- Eisen, J.S. and Melançon, E. (2001). Interactions with identified muscle cells break motoneuron equivalence in embryonic zebrafish. *Nat. Neurosci.* 4, 1065-70.

- Eisen, J.S., Myers, P.Z. and Westerfield, M. (1986). Pathway selection by growth cones of identified motoneurons in live zebra fish embryos. *Nature* 320, 269-71.
- Eisen, J.S., Pike, S.H. and Romancier, B. (1990). An identified motoneuron with variable fates in embryonic zebrafish. *J. Neurosci.* 10, 34-43.
- Flanagan-Steet, H., Fox, M.A., Meyer, D. and Sanes, J.R. (2005). Neuromuscular synapses can form in vivo by incorporation of initially aneural postsynaptic specializations. *Development* 132, 4471-81.
- Fricke, C. and Chien, C.-B. (2005). Cloning of full-length zebrafish *dcc* and expression analysis during embryonic and early larval development. *Dev. Dyn.* 234, 732-9.
- Hong, K., Hinck, L., Nishiyama, M., Poo, M.-M., Tessier-Lavigne, M. and Stein, E. (1999). A ligand-gated association between cytoplasmic domains of UNC5 and DCC family receptors converts netrin-induced growth cone attraction to repulsion. *Cell* 97, 927-41.
- Hutchinson, S.A., Cheesman, S.E., Hale, L.A., Boone, J.Q. and Eisen, J.S. (2007). Nkx6 proteins specify one zebrafish primary motoneuron subtype by regulating late *islet1* expression. *Development* 134, 1671-7.
- Kennedy, T.E., Wang, H., Marshall, W. and Tessier-Lavigne, M. (2006). Axon guidance by diffusible chemoattractants: a gradient of netrin protein in the developing spinal cord. *J. Neurosci.* 26, 8866-74.
- Kimmel, C.B., Ballard, W. W., Kimmel, S.R., Ullmann, B. and Schilling, T.F. (1995). Stages of embryonic development of the zebrafish. *Dev. Dyn.* 203, 253-310.
- Lauderdale, J.D., Davis, N.M. and Kuwada, J.Y. (1997). Axon tracts correlate with netrin-1a expression in the zebrafish embryo. *Mol. Cell. Neurosci.* 9, 293-313.
- Lu, X., Le Noble, F., Yuan, L., Jiang, Q., De Lafarge, B., Sugiyama, D., Breant, C., Claes, F., De Smet, F., Thomas, J.L. et al. (2004). The netrin receptor UNC5B mediates guidance events controlling morphogenesis of the vascular system. *Nature* 432, 179-86.
- Mawdsley, D.J., Cooper, H.M., Hogan, B.M., Cody, S.H., Lieschke, G.J. and Heath, J. K. (2004). The Netrin receptor Neogenin is required for neural tube formation and somitogenesis in zebrafish. *Dev. Biol.* 269, 302-15.

- Melançon, E., Liu, D.W., Westerfield, M. and Eisen, J.S. (1997). Pathfinding by identified zebrafish motoneurons in the absence of muscle pioneers. *J. Neurosci.* 17, 7796-804.
- Mitchell, K.J., Doyle, J.L., Serafini, T., Kennedy, T.E., Tessier-Lavigne, M., Goodman, C.S. and Dickson, B.J. (1996). Genetic analysis of Netrin genes in *Drosophila*: Netrins guide CNS commissural axons and peripheral motor axons. *Neuron* 17, 203-15.
- Moore, S.W., Correia, J.P., Lai Wing Sun, K., Pool, M., Fournier, A.E. and Kennedy, T.E. (2008). Rho inhibition recruits DCC to the neuronal plasma membrane and enhances axon chemoattraction to netrin 1. *Development* 135, 2855-64.
- Myers, P.Z., Eisen, J.S. and Westerfield, M. (1986). Development and axonal outgrowth of identified motoneurons in the zebrafish. *J. Neurosci.* 6, 2278-89.
- Nishiyama, M., Hoshino, A., Tsai, L., Henley, J.R., Goshima, Y., Tessier-Lavigne, M., Poo, M.-M. and Hong, K. (2003). Cyclic AMP/GMP-dependent modulation of Ca²⁺ channels sets the polarity of nerve growth-cone turning. *Nature* 423, 990-5.
- Park, K.W., Urness, L.D., Senchuk, M.M., Colvin, C.J., Wythe, J.D., Chien, C.-B. and Li, D.Y. (2005). Identification of new netrin family members in zebrafish: developmental expression of netrin 2 and netrin 4. *Dev. Dyn.* 234, 726-31.
- Rajasekharan, S. and Kennedy, T.E. (2009). The netrin protein family. *Genome Biol.* 10, 239.
- Shewan, D., Dwivedy, A., Anderson, R. and Holt, C.E. (2002). Age-related changes underlie switch in netrin-1 responsiveness as growth cones advance along visual pathway. *Nat. Neurosci.* 5, 955-62.
- Strahle, U., Fischer, N. and Blader, P. (1997). Expression and regulation of a netrin homologue in the zebrafish embryo. *Mech. Dev.* 62, 147-60.
- Suli, A. (2007). The axon guidance molecule Netrin is required in the guidance of dendrites and vascular endothelial cells.
- Suli, A., Mortimer, N., Shepherd, I. and Chien, C.-B. (2006). Netrin/DCC signaling controls contralateral dendrites of octavolateralis efferent neurons. *J. Neurosci.* 26, 13328-37.
- Trevarrow, B., Marks, D.L. and Kimmel, C.B. (1990). Organization of hindbrain segments in the zebrafish embryo. *Neuron* 4, 669-79.

- Varela-Echavarria, A., Tucker, A., Puschel, A.W. and Guthrie, S. (1997). Motor axon subpopulations respond differentially to the chemorepellents netrin-1 and semaphorin D. *Neuron* 18, 193-207.
- Welten, M.C., de Haan, S.B., van den Boogert, N., Noordermeer, J.N., Lamers, G.E., Spalink, H.P., Meijer, A.H. and Verbeek, F.J. (2006). ZebraFISH: fluorescent in situ hybridization protocol and three-dimensional imaging of gene expression patterns. *Zebrafish* 3, 465-76.
- Westerfield, M., McMurray, J.V. and Eisen, J.S. (1986). Identified motoneurons and their innervation of axial muscles in the zebrafish. *J. Neurosci.* 6, 2267-77.